TATION PAGE

Form Approved
OMB No. 0704-0188

I to average 1 hour per response, including the time for reviewing instructions, searching existing data sources, ewing the collection of information. Send comments regarding this burden estimate or any other aspect of this ion, to Washington Headquarters Services, Directorate for Information Operations and Reports, 1215 Jefferson ce of Management and Budget, Paperwork Reduction Project (0704-0188), Washington, DC 20503.

1. AGENCY USE ONLY (Leave blank)	2. REPORT DATE	3. REPORT TYPE AND DATES COVERED
	5 May 1992	Annual Technical 12/01/90 to 11/30/91

4. TITLE AND SUBTITLE

STUDIES OF OPTICAL BEAM PHASE-CONJUGATION & ELECTROMAGNETIC SCATTERING PROCESS

5. FUNDING NUMBERS

F49620-91-C-0018DEF

2

6. AUTHOR(S)

ROBERT W. HELLWARTH

7. PERFORMING ORGANIZATION NAME(S) AND ADDRESS(ES)

University of Southern California
Los Angeles, CA 90089

8. PERFORMING ORGANIZATION REPORT NUMBER

AFOSR-TR- 92 0435

9. SPONSORING/MONITORING AGENCY NAME(S) AND ADDRESS(ES)

Air Force Office of Scientific Research
Bolling Air Force Base, Building 410
Washington, D.C. 20332-6448

NE

10. SPONSORING/MONITORING AGENCY REPORT NUMBER

2301/A5

11. SUPPLEMENTARY NOTES

This document has been approved for public release and sale; its distribution is unlimited.

DTIC
ELECTE
JUN 22 1992
S D
A

12a. DISTRIBUTION/AVAILABILITY STATEMENT

unlimited

12b. DISTRIBUTION CODE

13. ABSTRACT (Maximum 200 words)

In this project we have performed both experimental and theoretical studies of optical beam phase-conjugation and of electromagnetic scattering and propagation with intense optical fields. We have: (1) made measurements of high-power four-wave mixing in many new polymers synthesized at USC to characterize their nonlinear optical properties; (2) made what we believe is the first observation of nonexponential attenuation of a weak optical beam in a homogeneous (highly scattering) medium; (3) achieved the first time-of-flight measurements of electron drift velocities in photorefractive insulating crystals, finding trap-limited room temperature mobilities ~ 0.2 $cm^2 V^{-1}s^{-1}$ and conduction band mobilities over an order of magnitude larger, also at room temperature; and (4) achieved the first low energy (~ picojoule) optical logic gates in resonant atomic vapors.

14. SUBJECT TERMS

Optical beam phase-conjugation. Nonlinear optics. High power optical beam propagation. Photorefractive effect.

15. NUMBER OF PAGES
22 + 6 Appendices

16. PRICE CODE

17. SECURITY CLASSIFICATION OF REPORT	18. SECURITY CLASSIFICATION OF THIS PAGE	19. SECURITY CLASSIFICATION OF ABSTRACT	20. LIMITATION OF ABSTRACT
UNCLASSIFIED		UNCLASSIFIED	

NSN 7540-01-280-5500

Standard Form 298 (Rev. 2-89)
Prescribed by ANSI Std. Z39-18

1. INTRODUCTION AND PROJECT OBJECTIVES

Nonlinear optics, the study of matter interactions with intense electromagnetic fields, has uncovered surprising and useful physical effects, such as stimulated scattering of light by which an intense monochromatic beam can be converted to intense coherent beams of different wavelengths. Recently, interesting processes involving nonlinear optical image–bearing beams have been discovered, such as optical–beam phase conjugation. Optical–beam phase conjugation is the name given to any process which generates, in real time, the time–reversed replica of a complex, image–bearing, optical beam, or which generates other related reflected beams, both monochromatic and polychromatic. Phase conjugation by optical four–wave mixing was conceived earlier in this project, as were such applications of phase–conjugation as the correction of image aberrations, brightness enhancement of laser outputs, edge–enhancement of images, automatic steering of beams, and optical spectroscopy by Raman–induced phase conjugation (RIPC). Such nonlinear optical techniques are currently being extended to perform many forms of beam processing, sorting, and routing on picosecond time scales. This project aims at exploring and developing these and other new wave–mixing processes, and the necessary nonlinear materials. Other novel electromagnetic scattering processes which occur at the intense optical fields available from lasers are also explored for their scientific and device interest. The approaches taken in this project are both experimental and theoretical.

2. MAJOR ACCOMPLISHMENTS: 12/1/90 to 11/30/91

The major accomplishments of this grant period were as follows.

2.1 Synthesis and Characterization of Optical Polymers

About four years ago in this AFOSR project, we began an effort to develop rugged and stable polymer films, both amorphous and crystalline, for nonlinear optical imaging or "real–time" holography. This effort is in collaboration with professor L. Dalton and his collaborators in the USC Chemistry Deparment who synthesize the materials and perform NMR and EPR studies on them. Our role in this project is to measure: (1) one– and two–photon absorption spectra, (2) film thickness using a step–profiler and electron microscopy, (3) the linear indices of refraction by reflectivity measurements, (4) space components of that part $C_{ijkl}(-\omega,\omega,\omega,-\omega)$ of the degenerate four–wave mixing susceptibility tensor that respond in a time less than 10 ps (our instrument resolution time) and to measure these vs ω, (5) the parameters which determine the slower–responding density and temperature gratings and the transient refractive index gratings which they create and (6) the third–harmonic light when it is visible. To date we have performed such measurements on films of several dozens of different polymers formed on glass microscope slides. We have reported results on over a dozen of the more interesting polymers in various publications in Sec. 3 and in the conference presentations (with published summaries) in Sec. 4. In the current period we have reported on refinements in the methods of synthesis and characterization, details of which are in Pubs 3.55 – 3.57. Pub. 3.55 is attached as Appendix I

and Pub 3.56 is attached as Appendix II.

A major accomplishment of our picosecond polymer studies has been the development of straightforward techniques for using picosecond pulse measurements of nonlinear material parameters that (1) allow meaningful comparison among results from different laboratories, (2) allow realistic estimates of uncertainties in the derived nonlinear parameters that arise from uncertainties in the transverse and longitudional pulse profiles, (3) allow full use of the sixteen independent combinations of the states of polarization of the four beams, and (4) allow unambiguous separation of the various timescales of the "slow" responding nonlinearities and the relative contribution of the "fast" (compared to pulse length) component. These techniques, used in Appendix I, are described at length in Pub. 3.44 in which we also note ambiguities in the previous literature which our technique can avoid.

Other accomplishments in polymer studies in the current period include succesful application of the phase conjugating Twyman–Green interferometer arrangement to measuring both the real and imaginary parts of C_{ijkl} tensor elements of polymers, as we described in Pubs. 3.56 and 3.57, the first of which is included here as Appendix II. We have also been able to measure nonlinear tensor elements as a function of wavelength from 515 to 720 nm, as shown in Appendix II.

2.2 Nonexponential Attenuation in Highly Scattering Homogenous Media; Artfical Kerr Media

We have made what we believe is the first observation of the nonexponential attenuation of a weak optical beam in a homogenous medium, that is, the first exception to the famous property of weak light beams that was first enunciated by Pierre Bouger 262 years

ago: "In a medium of uniform transparency the light remaining in a collimated beam is an exponential function of the length of its path in the medium." We expected such a violation would occur in our latex suspensions when the attenuation length due to scattering was of the order of (or shorter than) the correlation distance between the scattering particles. Our detailed theory fit the attenuation measurements well. Details are given in Pub 3.58 which is attached as Appendix III.

Our studies of nonexponential beam attenuation arose in the course of our longstanding project to study homogeneous suspensions and mixtures of non–absorbing particles. These media exhibit large optical nonlinearity (Kerr effect) by virtue of physical processes (such as molecular reorientation that also cause a large amount of light scattering. There is also the possibility that, if scattering is strong enough, randomly distributed localized light modes will form, similarly as "Anderson localization" of electronic states forms in random media. The nonexponential beam attenuation is related to light localization phenomena.

2.3 Physics of Photorefractive and Photoconducting Insulating Materials

In the current project period we achieved what we believe to be the first direct measurement of average drift velocity of photoexcited carriers in a photorefractive crystal (or in any insulator) in a known electric field. Details of these measurements and comparisons other published measurements are described in Pubs. 3.59 to 3.61 which are attached as Appendices IV, V, and VI. We outline these results below.

The drift velocities of photoexcited holes and electrons in known electric fields in insulators have long eluded direct experimental observation. Drift mobilities and carrier densities are generally too low to produce an observable Hall effect. Transient photoexcited

currents are observable but they have complex time envelopes, and carrier densities can only be guessed. Indirectly inferred values of the photo–excited electron mobility in single n–type $Bi_{12}SiO_{20}$ (n–BSO) crystals have ranged from around 10^{-5} to 10 $cm^2V^{-1}s^{-1}$ at room temperature. We have devised a holographic method to observe the movement of a grating of ($\sim 10^{12}$ cm^{-3}) photoexcited electrons as they drift in a known applied field. The application of this to n–BSO is described in Appendices IV, V, and VI. In Appendix IV we describe the new technique and report an electron mobility of 0.24 $\pm$ 0.07 $cm^2V^{-1}s^{-1}$ at room temperature. This value is so small as to suggest that the electrons spend considerable time in shallow traps while drifting toward their eventual recombination with a deep trap. With this in mind we were able to identify one portion of our observed transient photocurrent response with shallow–trap–limited drift, as we explain in Appendices V and VI. To pursue this idea further we are making direct time–of–flight holographic measurements of mobility over a temperature range (270 to 310 K) that show clear Arrhenius forms for shallow trap depths near 300 meV. A preliminary account of this work is in the published summary of Talk 4.113. We have also begun revising our time–of–flight measurement technique for the electron mobility so as to see the pure band conduction mobility on a short time scale after photoexcitation. In this case the shallow traps play no role. In Talk 4.11 a preliminary estimate 7 $\pm$ 3 $cm^2V^{-1}s^{-1}$ was given for this mobility in a well characterized sample of n–BSO.

We also made the first quantitative measurements of the spatial harmonic content of photorefractive gratings and compared these measurements with computer solutions of the standard model of photoexcitation, drift, diffusion and direct recombination of a single carrier species. These experiments were carried out in barium titanite. Preliminary results were reported in Talk 4.115.

In addition, we devised a novel grating technique to measure the optical properties of

the deep (ionized and occupied) traps from which the carriers are photo–excited. We call this technique "transport–induced–grating interferometry." Its application to the (unidentified) traps in cubic $Bi_{12}TiO_{20}$ was first outlined in Talk 4.116. Similar mesurements have been initiated to determine optical polarizabilities of cubic n–BSO. A preliminary account of first results of htese was given in Talk 4.117.

2.4 Atoms for logic

In the current project period, we began the studies we proposed of a wholly different class of nonlinear materials for image processing: thin cells of cesium or potassium vapor with special "buffering" by other vapors and by wall collisions. Preliminary accounts of our first successful vapor logic gates were given in Talks 4.118 to 4.121. Some possible applications of such nonlinear processes to the laser gravity–wave detector were discussed in Talk 4.122.

3. PAPERS AND Ph.D. THESES PUBLISHED FROM THIS PROJECT

3.1. "Theory of phase–conjugation in waveguides by four–wave mixing," R.W. Hellwarth, IEEE Journ. Quant. Elect., QE15, 101, February, 1979.

3.2. "Generation of time–reversed waves by nonlinear refraction in a waveguide," S.M. Jensen and R.W. Hellwarth, Appl. Phys. Lett., 33, 404, September, 1978.

3.3. "Infrared–to–optical image conversion by Bragg reflection from thermally–induced index gratings," G. Martin and R.W. Hellwarth, Appl. Phys. Lett., 34, 371, 1979.

3.4. "Spatial–diffusion measurements in impurity–doped solids by degenerate four–wave mixing," D.S. Hamilton, D. Heiman, Jack Feinberg, and R.W. Hellwarth, Optics Letters, 4, 124, 1979.

3.5. "Generation of time–reversed replicas of optical beams in barium titanate," Jack Feinberg, D. Heiman, and R.W. Hellwarth, Bulletin of the 1978 Annual Meeting of the Optical Society of America, 1367, October, 1978.

3.6. "Raman–induced Kerr Effect: A new laser–plasma diagnostic," M.V. Goldman and R.W. Hellwarth, Bull. Am. Phys. Soc., 2, 893, September, 1978.

3.7. "Conjecture on the effect of small anharmonicity on vibrational modes of glass," R.W. Hellwarth, Sol. State Comm., 32, pp.85–88, 1979.

3.8. "Photorefractive effects and light–induced charge migration in barium titanate," Jack Feinberg, D. Heiman, R.W. Hellwarth, and A. Tanguay, J. Appl. Phys., 51, pp.1297–1305, March, 1980.

3.9. "Generation of time–reversed replica of a nonuniformly polarized image–bearing optical beam," G. Martin, L.K. Lam, and R.W. Hellwarth, Optics Lett., 5, pp.185–187, May, 1980.

3.10. "Real–time edge enhancement using the photorefractive effect," Jack Feinberg, Optics letters, 5, pp.330–332, August, 1980.

3.11. "Four–wave mixing in photorefractive materials," Jack Feinberg and R.W. Hellwarth, Paper and Abstract E.3, Proceedings of XI International Conference on Quantum Electronics, Boston, Massachusetts, June 23–26, 1980.

3.12. "A wide–angle narrowband optical filter using phase–conjugation by four–wave mixing in a waveguide," L.K. Lam and R.W. Hellwarth, Abstract E.10, Proceedings of XI International Conference on Quantum Electronics, Boston, Massachusetts, June 23–26, 1980.

3.13. "High resolution resonance Raman spectroscopy of Iodine Vapor," D. Kirillov, and R.W. Hellwarth, Bull. Am. Phys. Soc., 25, No.9, p.1129, November, 1980.

3.14. "Pulsed phase conjugation due to a tensor refractive index grating in sodium vapor," S.N. Jabr, L.K. Lam and R.W. Hellwarth, Bull. Am. Phys. Soc., 25, No.9, p.1124, November, 1980.

3.15. "Phase–conjugation with nanosecond laser pulses in $BaTiO_3$," L.K. Lam, T.Y. Chang, Jack Feinberg and R.W. Hellwarth, Abstract, Bull. Optical Soc., Fall 1980 meeting, Chicago, Illinois.

3.16. "Phase–conjugating mirror with continuous–wave gain," Jack Feinberg and R.W. Hellwarth, Optics Letters, 5, pp.519–521, December, 1980.

3.17. "New component in degenerate four–wave mixing of optical pulses in sodium vapor," S.N. Jabr, L.K. Lam and R.W. Hellwarth, Phys. Rev. A, 24, pp.3264–3267, December, 1981.

3.18. "High resolution resonance Raman spectroscopy in the B–X band of I_2^{127} vapor," D. Kirillov, L.K. Lam, and R.W. Hellwarth, J. Molec. Spectroscopy, 91, pp.269–272,

January, 1982.

3.19. "Photorefractive index gratings formed by nanosecond optical pulses in $BaTiO_3$," L.K. Lam, T.Y. Chang, Jack Feinberg and R.W. Hellwarth, Optics Lett., 6, pp.475–477, October, 1981.

3.20. "Asymmetric self–defocusing of an optical beam from the photorefractive effect," Jack Feinberg, J. Opt. Soc. Am., 72, pp.46–51, January, 1982.

3.21. "Optical beam phase conjugation by stimulated backscattering," R.W. Hellwarth, Optical Engineering, 21, pp.263–266, March/April, 1982.

3.22. "Optical beam phase conjugation by four–wave mixing in a waveguide," R.W. Hellwarth, Optical Engineering, 21, pp.262–263, March/April, 1982.

3.23. "Observation of intensity–induced nonreciprocity in a fiberoptic gyroscope," S. Ezekiel, J.L. Davis, and R.W. Hellwarth, Proc. of International Conference on Fiberoptic Rotation Sensors (M.I.T., November 9–11, 1981), edited by S. Ezekiel (Springer–Verlag, New York, Mew York, 1982).

3.24. "Observation of intensity–induced nonreciprocity in a fiber optic gyroscope," S. Ezekiel, J.L. Davis, and R.W. Hellwarth, Optics Lett., 7, pp.457–459, September, 1982.

3.25. "Optical beam phase conjugation by stimulated backscattering in multimode optical waveguides," R.W. Hellwarth, in New Direction in Guided Waves and Coherent Optics, Vol.II, pp.335–357, edited by D.B. Ostrowsky and E. Spitz (Martinus Nijhoff Pub., Boston, Massachusetts, 1984).

3.26. "Raman–induced phase conjugation spectroscopy," S.K. Saha and R.W. Hellwarth, Phys. Rev. A, 27, pp.919–922, February, 1983.

3.27. "Phase conjugation by stimulated backscattering," R.W. Hellwarth, Chapter 7 of Optical Phase Conjugation, edited by R.A. Fisher (Academic Press, New York, New York, 1983).

3.28. "Phase conjugation by four–wave mixing in a waveguide," R.W. Hellwarth, Chapter 5 of Optical Phase Conjugation, edited by R.A. Fisher (Academic Press, New York, New York, 1983).

3.29 "Holographic time–resolved measurements of bulk space–charge gratings in photorefractive bismuth silicon oxide," R.A. Mullen. Thesis presented for Ph.D. in Electrical Engineering, December 7, 1983.

3.30 "Image processing using nonlinear optical effects," R.W. Hellwarth, in Optical Nonlinearities, Fast Phenomena and Signal Processing, edited by N. Peyghambarian (National Science Foundation, Washington, D.C., 1986).

3.31 "Minimum power requirements for efficient four–wave mixing and self–focusing of electromagnetic beams in glasses and fluids," R.W. Hellwarth, Phys. Rev. A, 31, pp.533–536, January, 1985.

3.32 "Optical measurements of the photorefractive parameters of $Bi_{12}SiO_{20}$" R.A. Mullen and R.W. Hellwarth, Journ. Appl. Phys., 58, pp.40–44, July, 1985.

3.33 "Optical phase conjugation by backscattering in barium titanate," T.Y. Chang and R.W. Hellwarth, Optics Lett., 101, pp.408–410, August, 1985.

3.34 "Hole–electron competition in photorefractive gratings," F.P. Strohkendl, J.M.C. Jonathan, and R.W. Hellwarth, Optics Lett., 11, pp.3122–314, May, 1986.

3.35 "Effect of applied electric field on the buildup and decay of photorefractive gratings," J.M.C. Jonathan, R.W. Hellwarth, and G. Roosen, IEEE Journ. Quantum Electronics, QE–22, pp. 1936–1941, October, 1986.

3.36 "Image processing using nonlinear optical effects," R.W. Hellwarth, pp.67–69, in Optical Nonlinearities, Fast Phenomena and Signal Processing, edited by N. Peyghambarian (National Science Foundation, Washington, 1986).

3.37 "Contribution of holes to the photorefractive effect in n–type $Bi_{12}SiO_{20}$," F.P. Strohkendl and R.W. Hellwarth, J. Appl. Phys., 62, pp.2450–2455, September, 1987.

3.38 "Photorefractive and liquid crystal materials," P. Brody, U. Efron, J. Feinberg, A. Glass, R.W. Hellwarth, R. Neurogaonkar, G. Rakuljic, C. Valley and C. Woods, Appl. Opt., 26, pp.220–224, January, 1987.

3.39 "Theory and observation of electron–hole competition in the photorefractive effect," R.W. Hellwarth, in Laser Optics of Condensed Matter, ed. by J.L. Birman, H.Z. Cummins, and A.A. Kaplyanskii (Plenum Press, New York, New York, 1988).

3.40 "Experimental observation of plasma wake–field acceleration," J.B. Rosenzweig, D.B. Cline, B. Cole, H. Figueroa, W. Gai, R. Konecny, J. Norem, P. Schoessow, and J. Simpson, Phys. Rev. Lett., 61, p.98, 1988.

3.41 "Direct measurement of beam–induced fields in accelerating structures," H. Figueroa, W. Gai, R. Konecny, J. Norem, A. Ruggiero, P. Shoessow, and J. Simpson, Phys. Rev. Lett., 60, 2144 (1988).

3.42 "Nonlinear index of air at 1.053μm," D.M. Pennington, M.A. Henesian, and R.W. Hellwarth, Phys. Rev. A, 39, pp.3003–3009, March, 1989.

3.43 "Comment on 'reflected phase–conjugate wave in a plasma'," R.W. Hellwarth, D. Lininger, and M.V. Goldman, Phys. Rev. Lett., Vol.62, p.3011, June, 1989.

3.44. "Picosecond nonlinear optical response of three rugged polyquinoxaline–based aromatic conjugated ladder–polymer thin films," X.F. Cao, J.P. Jiang, D.P. Bloch, R.W. Hellwarth, L.P. Yu, and L. Dalton, J. Appl. Phys., Vol.65, pp.5012–5018, June, 1989.

3.45. "Studies of materials and configurations for optical beam phase conjugation," David L. Naylor. Ph.D. thesis (Electrical Engineering) University of Southern California, May, 1988.

3.46. 'Photorefractive hole–electron competition, light–induced dark decays, and photorefractive effect in $Bi_{12}SiO_{20}$," Friedrich P. Strohkendl. Ph.D. thesis (Physics) University of Southern California, May, 1988.

3.47. "Nonlinear optical studies of photorefractive barium titanate: parameter measurments and phaseconjugation", T. Y. Chang, Ph.D. Thesis (Electrical Engineering) University of Southern California, December, 1986.

3.48. "Characterization and modeling of the photorefractive effect in bismuth silicon oxide", P. Tayebati, Ph.D. Thesis (Physics) University of Southen California, May, 1989.

3.49. "Studie. of photorefractive effect in barium titanate: higher order spatial harmonics and two beam energy coupling", Y. H. Lee, Ph.D. Thesis (Electrical Engineering) University of Southern California, May, 1989.

3.50. "Comparative study of photorefractive $Bi_{12}SiO_{20}$ crystals", F. P. Strohkendl, P. Tayebati, and R. W. Hellwarth, J. Appl. Phys., vol. 66, pp. 6024–6029, December, 1989.

3.51. "Light–induced dark decays of photorefractive gratings and their observation in $Bi_{12}SiO_{20}$", F. P. Strohkendl, J. Appl. Phys., vol. 65, pp. 3773–3779, March, 1989.

3.52. "Recent advances in the synthesis of new nonlinear optical polymers", L. P. Yu, R. Vac, L. R. Dalton, and R. W. Hellwarth, Proc. S. P. I. E., vol. 1147, pp. 142–148, 1989.

3.53. "Indices governing optical self–focusing and self–induced changes in the state of polarization in N_2, O_2, H_2 and Ar gases" R. W. Hellwarth, D. M. Pennington and M. A. Henesian, Phys. Rev. A, vol. 41, pp. 2766–2777, March, 1990.

3.54. "Picosecond laser studies of third order nonlinear optical properties in organic polymers", X. F. Cao, Ph.D. Thesis (Physics) University of Southern California, May, 1990.

3.55. "Synthesis and characterization of third order nonlinear optical materials," L.P. Yu, M. Chen, L.R. Dalton, X.F. Cao, J.P. Jiang, and R.W. Hellwarth, Materials Res. Soc. Symp. Proc. vol. 173, pp. 607–612 (1990).

3.56. "Bipolaronic enhanced third order nonlinearity in organic ladder polymers," X.F. Cao, J.P. Jiang, R.W. Hellwarth, L.P. Yu, M. Chen, and L.R. Dalton, S.P.I.E. vol. 1337, pp. 114–124 (1990).

3.57. "Four wave mixing in photorefractive and polymeric materials: ring phase conjugator and time–resolved measurement of third order optical nonlinearity," Jien–Ping Jiang, Ph.D. Thesis (Physics), USC, Dec. 1990.

3.58. "Anomalous optical transmission in homogenous latex suspensions," P. Tam, and R.W. Hellwarth, Phys. Rev. B, vol. 43, pp. 13314–13319, June 1991.

3.59. "Direct determination of electron mobility in photorefractive $Bi_{12}SiO_{20}$ by a holographic time–of–flight technique," J.P. Partanen, J.M.C. Jonathan, and R.W. Hellwarth, Appl. Phys. Lett., vol. 57, pp. 2404–2406, Dec. 1990.

3.60. "Charge transport and holographic determination of the mobility of the charge carriers in photorefractive BSO", J.P. Partanen, P. Nouchi, J.M.C. Jonathan, and R.W. Hellwarth, Annales de Physique, Colloque no 1, Supplement au no 1, vol. 16, pp. 135–142, Feb. 1991.

3.61. "Comparison between holographic and transient–photocurrent measurements of electron mobility in photorefractive $Pi_{12}SiO_{20}$," J.P. Partanen, P. Nouchi, J.M.C. Jonathan, and R.W. Hellwarth, Phys. Rev. B, vol. 44, pp. 1487–1491, Jyly 1991.

4. TALKS, SEMINARS, WORKSHOPS AND CONFERENCES STEMMING FROM THIS PROJECT

4.1 "Optical image processing and computing," Physics Department Seminar, California Institute of Technology, Pasadena, California, 3 May 1983.

4.2 "Band transport model of photorefractive materials with two photoactive levels," G.C. Valley, R.A. Mullen, and R.W. Hellwarth, paper TUM 33, Conference on Lasers and Electro–optics CLEO'83 Technical Digest, p.74 (Optical Society of America, Washington, D.C., 1983).

4.3 "Wide–angle narrowband optical filter using phase conjugation by stimulated Brillouin scattering," S.K. Saha and R.W. Hellwarth, paper THC4, Conference on Lasers and Electro–optics, Baltimore, Maryland, 19 May 1983. Summary published in CLEO'83 Technical Digest, pp.158–160 (Optical Society of America, Washington, D.C., 1983).

4.4 "Double exponential decay of photorefractive gratings in $Bi_{12}SiO_{20}$," R.A. Mullen and R.W. Hellwarth, paper THH3, Conference on Lasers and Electro–optics, Baltimore, Maryland, 19 May 1983. Summary published in CLEO'83 Technical Digest, p. 174 (Optical Society of America, Washington, D.C., 1983).

4.5 "The photorefractive effect for phase conjugation," R.W. Hellwarth, Optics Group Seminar, Royal Signals and Radar Establishment, Gt. Malvern, England, 21 June 1983.

4.6 "Stimulated Brillouin scattering: A collective mode," R.W. Hellwarth, Many–body Seminar, Universite Libre de Bruxelles, Brussels, Belgium, 1 July 1983.

4.7 "Optical beam phase conjugation: A review," R.W. Hellwarth, Physics Seminar,

University of Paris VI, 15 July 1983.

4.8 "Sound damping and non–propagating index fluctuations in optical glasses," R.W. Hellwarth, Solid State Seminar, Clarendon Laboratory, Oxford, 24 July 1983.

4.9 "Optical beam phase conjugation: A review," Physics Department, University of New Mexico, Albuquerque, New Mexico, 11 November 1983.

4.10 "Stimulated Brillouin and Raman scattering," R.W. Hellwarth, Hughes Aircraft Company, Electro–optical and Data Systems Group Seminar, 9 December 1983.

4.11 "Non–reciprocal phase shifts from the photorefractive effect," R.W. Hellwarth, Conference on Physics of Optical Ring Gyros, Snowbird, Utah, 8 January 1984.

4.12 "Error in phase conjugation by stimulated Brillouin scattering," R.W. Hellwarth, 14th Winter Colloquium on Quantum Electronics, Snowbird, Utah, 12 January 1984.

4.13 "Optical beam phase conjugation: A review," R.W. Hellwarth, Institut d'Optique, Orsay, France, 19 April 1984.

4.14 "Phase–conjugation for physical measurement," R.W. Hellwarth, Ecole Normale Superieur, Paris, France, 24 May 1984.

4.15 "The photorefractive effect," R.W. Hellwarth, University of Paris Nord, Paris, France, 15 May 1984.

4.16 "The photorefractive effect: Physics and applications to optical image processing," R.W. Hellwarth, Institut d'Optique, Orsay, France, 17 May 1984.

4.17 "Use of phase conjugation for physical measurement," R.W. Hellwarth, Institut d'Optique, Orsay, France, 29 May 1984.

4.18 "Use of phase conjugation for physical measurement," R.W. Hellwarth, Invited paper ThAA1, XIII International Conference on Quantum Electronics, Anaheim, California, 21 June 1984.

4.19 "Effect of applied electric field on the buildup and decay of photorefractive gratings," J.M. Cohen–Jonathan, R.W. Hellwarth, and G. Roosen, 1984 Annual Meeting of the Optical Society of America, San Diego, California, 31 October 1984, Abstract WBI Technical Program, p. P35.

4.20 "One–way image transmission and reconstruction through a distorting medium," T.Y. Chang and Paul Nachman, paper TuA2, Annual Meeting of the Optical Society of America, 30 October 1984.

4.21 "Phase conjugation, problems and limitations," R.W. Hellwarth, TRW Applied Technology Division Seminar, 10 October 1984.

4.22 "Physics of optical beam phase conjugation," R.W. Hellwarth, Columbia University Physics Colloquium, 28 September 1984.

4.23 "Physical limits for phase conjugation and self–focusing of electromagnetic waves," R.W. Hellwarth, Aerospace Corporation Seminar, 29 August 1984.

4.24 "Physical limits to optical phase conjugation," R.W. Hellwarth, 15th Winter Colloquium on Quantum Electronics, Snowbird, Utah, 11 January 1985.

4.25 "Minimum power requirements for efficient four–wave mixing and self–focusing of electromagnetic beams in glasses and fluids," R.W. Hellwarth, Electrical Engineering Colloquium, Ohio State University, Columbus, Ohio, 28 January 1985.

4.26 "Optical phase conjugation: A review," R.W. Hellwarth, Winter College on Lasers, Atomic and Molecular Physics, International Centre for Theoretical Physics, Trieste, Italy, 10 February, 1985.

4.27 "Phase–conjugation, pulse shortening, and frequency shifting of optical beams by stimulated scattering," R.W. Hellwarth, ibid., 11 February 1985.

4.28 "The photorefractive effect: Physics and applications to optical image processing," R.W. Hellwarth, ibid., 12 February 1985.

4.29 "Use of phase conjugation for physical measurement," R.W. Hellwarth, ibid., 13 February 1985.

4.30 "Minimum energy requirements for optical logic," R.W. Hellwarth, Instituto di Ottica, Florence, Italy, 19 February 1985.

4.31 "Phase conjugation: A review," R.W. Hellwarth, Instituto di Elettronica Quantistica, Florence, Italy, 20 February 1985.

4.32 "Photorefractive measurements," R.W. Hellwarth, Instituto di Ricerce Onde Elettromagnetiche, Florence, Italy, 21 February 1985.

4.33 "Phase conjugation for four–wave mixing in optical waveguides," R.W. Hellwarth, Physics Colloquium, University of Rome, Rome, Italy, 26 February 1985.

4.34 "Physical limits on logic operations employing nonlinear optical effects," R.W. Hellwarth, paper MC2 at the Winter '85 Topical Meeting on Optical Computing, Incline Village, Nevada, 18 March 1985. Abstract and Summary in Proceedings.

4.35 "Use of optical phase conjugation for understanding basic materials properties," R.W. Hellwarth, Topical Conference on Basic Properties of Optical Materials, National Bureau of Standards, Gaithersburg, Maryland, 9 May 1985. Summary paper published in Basic Properties of Optical Materials, NBS Special Publication 697, edited by A. Feldman (U.S. Government Printing Office, Washington, D.C., 1985).

4.36 "Optical measurements of densities, lifetimes, cross sections and species of charge carriers in insulators and semiconductors," R.W. Hellwarth, Physics Departmental Seminar, Columbia University, New York, New York, 15 November 1985.

4.37 "Fundamental limits on energies and power required for nonlinear optical effects,"

R.W. Hellwarth, Physics Departmental Seminar, Columbia University, New York, New York, 20 November 1985.

4.38 "Anomalous cross–sections and phase conjugation in optical backscattering," R.W. Hellwarth, Resonance Seminar, Columbia University, New York, 22 November 1985.

4.39 "The photorefraction effect: Physics and application," R.W. Hellwarth, Applied Physics Seminar, Columbia University, New York, New York, 26 November 1985.

4.40 "Optical measurements of electrons and holes in insulators," R.W. Hellwarth, AT&T Bell Laboratories Research Seminar, Murray Hill, New Jersey, 27 November 1985.

4.41 "Determination of electron and hole parameters in insulators," R.W. Hellwarth, Research Seminar, Philips Research Laboratories, Briarcliff Manor, New York, 10 December 1985.

4.42 "Optical measurements of the properties of photorefractive impurities for device design" R.W. Hellwarth, Invited talk at the Materials Research Society 1985 Annual Meeting, Boston, Massachusetts, 4 December 1985.

4.43 "Photorefractive materials and devices," R.W. Hellwarth, USC Engineering Research Review, Los Angeles, California, 2 April 1985.

4.44 "Fundamental limits on nonlinear optical materials and processes," R.W. Hellwarth, Optical Society of America Workshop on Nonlinear Materials, Annapolis, Maryland, 28 April 1986. Summary in Applied Optics.

4.45 "Fundamental limits on energy and power required for nonlinear optical effects," R.W. Hellwarth, USC School of Engineering, 5th Annual Research Review, Los Angeles, California, 6 May 1986.

4.46 "Photorefractive measurements of anisotropy of the mobility of photo–excited holes in $BaTiO_3$," by C.P. Tzou, T.Y. Chang, and R.W. Hellwarth, paper 613–11, 21 January 1986, Los Angeles, California. Summary published in SPIE Proceedings, 613, p.58, March, 1986.

4.47 "Artificial Kerr Media," David Naylor, USC Engineering Department Seminar, Los Angeles, California, 25 July, 1986.

4.48 "Stimulated optical scattering from electron plasma," R.W. Hellwarth, Los Alamos National Laboratory Seminar, Los Alamos, New Mexico, 25 August 1986.

4.49 "Image processing materials," R.W. Hellwarth, Physics Seminar, University of New Mexico, Albuquerque, New Mexico, 28 August 1986.

4.50 "Image processing using nonlinear optical effects," R.W. Hellwarth, NSF Workshop on Optical Nonlinearities, Fast Phenomena, and Signal Processing, University of Arizona, Tucson, Arizona, 21 May 1986. Complete manuscript published in volume

of selected papers, Optical Nonlinearities Fast Phenomena and Signal Processing, edited by N. Peyghambarian (National Science Foundation, Washington, D.C., 1986).

4.51 "Characterization of photorefractive materials," R.W. Hellwarth, Physics Department, University of Amsterdam, Amsterdam, Holland, 1 June 1986.

4.52 "Fundamental limits of power and energy for nonlinear optical effects," R.W. Hellwarth, Institut d'Optique, Orsay, France, 6 June 1986.

4.53 "Optical implementation of cellular automata," R.W. Hellwarth, Physics Department, University of Paris, Place Jussieu, Paris, France, 8 June 1986.

4.54 "Raman–induced phase–conjugation spectroscopy," R.W. Hellwarth, University of Paris, Nord, Paris, France, 13 June 1986.

4.55 "An optical associative memory," R.W. Hellwarth, Max–Planck–Institut für Quantenoptik, Munich, West Germany, 19 June 1986.

4.56 "An optical associative memory," R.W. Hellwarth, Optical Parallel Computing Conference, Utah State University, Logan, Utah, 14 October 1986.

4.57 "Fundamental limits on optical computing," R.W. Hellwarth, Optical Parallel Computing Conference, Utah State University, Logan, Utah, 15 October 1986.

4.58 "Hole–electron competition in photorefractive gratings," F.P. Strohkendl, J.M.C. Jonathan, and R.W. Hellwarth, Paper FQ2 with published abstract. 1986 Conference on Lasers and Electro–optics (CLEO), San Francisco, California, 13 June 1986. Abstract in Digest of Technical Papers, pp.386–387, published by the Optical Society of America, Washington, D.C., 1986.

4.59 "Hole contributions to the photorefractive effect in n–type $Bi_{12}SiO_{20}$," F.P. Strohkendl and R.W. Hellwarth, Paper WG17 at the 1986 Annual Meeting of the Optical Society of America, Seattle, Washington, 22 October 1986. Abstract published in the Technical Digest, p.81, published by the Optical Society of America, Washington, D.C., 1986. Short abstract in Optics News, 12, No.9, p.162, September, 1986.

4.60. "A comparative study of the photorefractive effect in $Bi_{12}SiO_{20}$," F.P. Strohkendl, P. Tayebati, and R.W. Hellwarth, Paper WG17 at the Topical Meeting on Photorefractive Materials, Effects and Devices, August 12–14, 1987, Los Angeles, California. Summary published in Technical Digest Series, 17, pp.32–34, published by the Optical Society of America, Washington, D.C., 1987.

4.61. "Spatial harmonics of a photorefractive grating induced by sinusoidal optical intensity variation in a $BaTiO_3$ crystal," Y.H. Lee and R.W. Hellwarth, at the Topical Meeting on Photorefractive Materials, Effects and Devices, August 12–14, 1987, Los Angeles, California. Summary published in Technical Digest Series, 17, pp.64–65, published by the Optical Society of America, Washington, D.C., 1987.

4.62. "Nonlinear refractive–index measurements of air and argon gases at 1 atm," D.M.

Pennington, M.A. Henesian, C.D. Swift, and R.W. Hellwarth, 1987 Annual Meeting of the Optical Society of America, 19 October 1987, Rochester, New York. Summary M16 of Technical Digest, 22, p.28, published by the Optical Society of America, Washington, D.C., 1987.

4.63. "Measurements of anisotropy of parameters in photorefractive barium titanate," T.Y. Chang R.W. Hellwarth, Conference on Lasers and Electro–optics (CLEO), Baltimore, Maryland, 29 April 1987. Summary published in Technical Digest Series, 14, pp.180–181, published by the Optical Society of America, Washington, D.C., 1987.

4.64. "Stimulated Brillouin scattering in plasmas," R.W. Hellwarth, Los Alamos Scientific Laboratory, Los Alamos, New Mexico, 5 August 1987.

4.65. "Photorefractive effect in $Bi_{12}SiO_{20}$," F.P. Strohkendl and R.W. Hellwarth, at the Review of Optical Computing and Photonics, University of Southern California, Los Angeles, California, 23 March 1987.

4.66. "Anomalous backscattering from random media," P. Tam and R.W. Hellwarth, at the Review of Optical Computing and Photonics, University of Southern California, Los Angeles, California, 23 March 1987.

4.67. "Cellular automata and optical computing," R.W. Hellwarth, IEEE Student Seminar, University of Southern California, Los Angeles, California, 18 November 1987.

4.68. "Optical devices for neural engineering," R.W. Hellwarth, Center for Neural Engineering (USC) Seminar, University of Southern California, Los Angeles, California, 19 November 1987.

4.69 "Overview of phase conjugate optics," R.W. Hellwarth, 18th Winter Colloquium on Quantum Electronics, Snowbird, Utah, 8 January 1988.

4.70 "Fidelity of optical phase conjugation by photorefractive degenerate four wave mixing in barium titanate," D.L. Naylor, Quantum Electronics Seminar, University of Southern California, 8 February 1988.

4.71. "Cellular automata simulations with nonlinear imaging," R.W. Hellwarth. 1988 Winter Meeting of IEEE/LEOS, Los Angeles Chapter, University of Southern California, 25 February 1988.

4.72. "Optical studies of charge transport in insulators," R.W. Hellwarth, University of Chicago, Physics Department Seminar, Chicago, Illinois, 7 April 1988.

4.73. "Picosecond nonlinear optical response of polymeric disubstituted ethylaminovinyl–polyaniline (pDEAVPA)," D.F. Bloch, X.F. Cao, R.W. Hellwarth, and J.P. Jiang, paper WW2 at the 1988 Conference on Lasers and Electrooptics. 27 April 1988 at Anaheim, California. Abstract in Conference Bulletin. Summary published in Technical Digest, Conference on Lasers and Electro–Optics (Optical Society of America, Washington, D.C., 1988). Paper WW2.

4.74. "Fidelity of optical phase conjugation by photorefractive degenerate four–wave mixing in $BaTiO_3$," D.L. Naylor and R.W. Hellwarth, paper TuG4 at the 1988 Conference on Lasers and Electrooptics, 26 April 1988 at Anaheim, California. Abstract in Conference Bulletin. Summary published in Technical Digest, Conference on Lasers and Electro–Optics (Optical Society of America, Washington, D.C., 1988). Paper TuG4.

4.75. "Backscattering from non–absorbing liquid suspensions," R.W. Hellwarth, Max Planck Institut für Quantenoptik (MPQ) Garching, West Germany, 19 May 1988.

4.76. "Anomolous photoconductivity in $Bi_{12}SiO_{20}$," R.W. Hellwarth, University of Crete, Heraklion, Greece, 6 June 1988.

4.77. "Electron–hole competition in photorefractive effects," R.W. Hellwarth, Institut d'Optique, Orsay, France, 13 June 1988.

4.78. "Stimulated optical scattering from an electron plasma," R.W. Hellwarth, University of Paris VI, Place Jussieu, Paris, France, 16 June 1988.

4.79. "Materials for modern optics," R.W. Hellwarth: 38th Meeting, Nobelpreistrager in Lindau, Lindau, West Germany, 29 June 1988.

4.80. "A plasma lens with highly stable properties," G.F. Kirkman, H. Figueroa, and M.A. Gundersen, American Physical Society Division of Plasma Physics Meeting, Florida, October 1988.

4.81. "Numerical observation of the Bragg effect on the propagation of electromagnetic waves," R. Keinings, Y.T. Yan, K. Akimoto, J.M. Dawson, H. Figueroa, and C. Joshi, American Physical Society Division of Plasma Physics Meeting, Florida, October 1988.

4.82. "The photorefractive effect in nonlinear optics", R. W. Hellwarth, Max Planc Institut fur Quantenoptik, Garching, FGR, 5 November 1988.

4.83. "Charge transport in sillenite crystals", R. W. Hellwarth, University of Zurich – ETH, Zurich, Switzerland, 10 November 1988.

4.84. "A plasma lens with highly stable properties", Conference on Advanced Accelerator Concepts, Lake Arrowhead, 9 January 1989, AIP Conference Proceedings No. 193, pp. 217–226 (Am. Ins. of Physics, New York 1989).

4.85. "Picosecond laser studies of anomalous sound damping in an amorphous polyquinoxaline layer", X. F. Cao, J. P. Jiang, D. F. Bloch, and R. W. Hellwarth, 25 April 1989, Paper TUGG28 at the Conference on Quantum Electronics and Laser Science 1989 in Baltimore, Md, Summary in: Technical Digest Series 1989, vol. 12, p. TUGG28 and three figures (Optical Soc. of Am. Washington, D.C. 1989).

4.86 "Discrepancy between the values of photoconductivity measured directly and the value predicted from holographic measurements in $Bi_{12}SiO_{20}$", P. Tayebati, and R. W. Hellwarth, Conference on Lasers and Electro–Optics, Summary in: Technical

Digest Series 1989, vol. 11, paper TUS5 (Opt. Soc. of Am., Washington, D.C. 1989).

4.87. "Measurement of two photon absorption by Cr–phthalocyanine in a polycarbonate film", J. P. Jiang, R. W. Hellwarth, L. P. Yu, and L. Dalton, 1989 Meeting of the Optical Society of America, October 19, 1989, Orlando, Fla, Summary in: Technical Digest Series, vol. 18, p. PD18, (publ. by Opt. Soc. of Am., Washinton, D.C. 1989)

4.88. "Synthesis and Characterization of Third–Order Nonlinear Optical Materials",L.P. Yu, M. Chen, L.R. Dalton, X.F. Cao, J.P. Jiang, and R.W. Hellwarth. at the Materials Research Society Symposium on Multi–Functional Materials" Boston, Mass., 29 Nov. 1989. Summary in Conference Proceedings.

4.89 "Propagation without diffraction?" R.W. Hellwarth, Institute Seminar, Institute of Optics, Florence, Italy, 28 February 1989.

4.90 "Alteration of transition frequencies and linewidths of atoms near objects", R.W. Hellwarth, Departmental Seminar, Universtiy of Rome–Sapienza, Rome, Italy, 7 March 1989

4.91 "Gain without inversion", R.W. Hellwarth, Seminar, Max Planck Institut fur Quantenoptik, Garching West Germany, 17 Feb 89.

4.92 "Photorefractive Optics", R. W. Hellwarth, Institute of Optics, Orsay, France, 18 May 1989.

4.93 "Optical Cellular Automata", R.W. Hellwarth, University of Paris–Jussieu, 22 May 1989.

4.94 "Subnatural linewidths", R.W. Hellwarth, Laboratoire de Physique des Lasers, Un. of Paris Nord, 24 May 1989.

4.95 "Recent advances in the synthesis and characterization of new nonlinear optical polymers", L.P. Yu, R.Vac, L.R. Dalton, and R.W. Hellwarth, S.P.I.E. Symposium on Nonlinear Optical Properties of Organic Materials II, San Diego, Calif., 10 August 1989. Summary in Conference Proceedings.

4.96 "Measurement of Two–Photon Absorption by Cr–phthalocyanine in polycarbonate film", J.P. Jiang, X.F. Cao, R.W. Hellwarth, L.P. Yu, and L. Dalton, Conference for Photonic Technology Review, USC, 14 Nov 1989.

4.97 "Non–exponential Optical Beam Attenuation in Homogeneous Media", P.W. Tam and R.W. Hellwarth, Center for Photonic Technology Review, USC, 14 Nov 1989.

4.98 "The limitations of Nonlinear Optical Devices", R.W. Hellwarth, Center for Photonic Technology Review, 14 Nov 1989.

4.99 "Limits to Optical Computing", R.W. Hellwarth, Quantum Electronics Seminar, USC, 15 Nov 1989.

4.100 "Subnatural Absorption Linewidths of Optical Transitions", Physics Colloquium, USC, 9 Oct 1989.

4.101. "Effects of Temperature on Photoconductivity in n–Type Cubic $Bi_{12}SiO_{20}$", J.P. Partanen, P. Nouchi, J.M.C. Jonathan and R.W. Hellwarth, Topical Meeting on Photorefractive Materials, Effects, and Devices II, CNRS Center, Aussois, France, 17 Jan 1990. Summary published in Technical Digest of the Topical Meeting on Photorefractive Materials, Effects, 2nd Devices II, pp. 109–11 (Opt. Soc. America, Washington, DC, 1990).

4.102. "Temperature dependence of photoconductivity in n–type $Bi_{12}SiO_{20}$", P. Nouchi, Laboratoire de Chimie du Solide du CNRS, 351, cours de la Liberation, 33400 Talence, France, 10 Jan 1990.

4.103. "Temperature effects on photorefractivity in n–type $Bi_{12}SiO_{20}$", P. Nouchi, Groupe d'Optique Nonlineaire et d'Optoelectronique, University of Strasbourgh, 5 rue de l'Universite, 67084 Strasbourg, Cedex F, France, 15 Jan 1990.

4.104. "Anomalous Optical Transmission in Homogeneous Latex Suspensions", P.W. Tam and R.W. Hellwarth, Conference on Lasers and Electrooptics 1990, Technical Digest Series, vol. 7 (Opt.Soc. America, Washington, DC 1990), pp 516–518. Abstract CFJ1, 25 May 1990.

4.105. "Second–Harmonic Generation in Laser–Assisted Poled Polymeric Materials", X.F. Cao, L.P. Yu, and L.R. Dalton", in OSA Annual Meeting Technical Digest 1990, vol. 15 of the OSA Technical Digest Series (Optical Soc. Am., Washington, DC 1990) p. 165.

4.106. "Progress in Modern Optics", R.W. Hellwarth, Graduate Student Seminar, USC, 18 Oct 1990.

4.107. "Atoms Near Dielectric Boundaries" R.W. Hellwarth, Seminar, Laboratoire de Physique des Lasers, 93430 Villeteneuse, France, 15 Jun 1990.

4.108. "Holographic Measurement of Electron Mobility in $Bi_{12}SiO_{20}$" R.W. Hellwarth, Seminar, Institut d'Optique, Orsay, France, 15 Jun 1990.

4.109. "Nonexponential Optical Attenuation in Homogeneous Media", R.W. Hellwarth, Seminar, Max Planck Institut fur Quantenoptik, D8046 Garching, Germany. 16 July 1990.

4.110. "Optical Attenuation in Highly Scattering Media", R.W. Hellwarth, Seminar at Naturrkundig Laboratorium, Amsterdam, Holland, 2 July 1990.

4.111. "Direct Determination of the Electron Mobility in Photorefractive $Bi_{12}SiO_{20}$ by a Holographic Technique", J.P. Partanen, J.MC. Jonathan, and R.W. Hellwarth, The IEEE/OSA Conference on Nonlinear Optics: Phenomena and Devices, Kauai, Hawaii. Paper ThP6, 19 July 1990. Summary published on p. 261 of "Nonlinear optics: Digest (IEEE Catalog No.90CH2905–8, New York, 1990).

4.112. "A Direct Holographic Measurement of Electron Mobility in Photorefractive

$Bi_{12}SiO_{20}$", J.P. Partanen, P. Nouchi, J.M.C. Jonathan, and R.W. Hellwarth, 6th Workshop of the French" Club Optique dans l'Ordinateur" on Optical Functions in Computers, 6 Sept 1990, Strassbourg, France.

4.113. "Temperature dependence of electron mobility in photorefractive $Bi_{12}SiO_{20}$", P. Nouchi, J.P. Partanen, and R.W. Hellwarth, paper CWD4 at the CLEO/QELS'91 Conference, Baltimore, MD, May 15 1991, Published in Conference on Lasers and Electro–Optics 1991, 1991 Tecnical Digest Series vol. 10, (Opt. Soc. Am., Washington, DC, 1991) pp. 234–235.

4.114. "Conduction band and trap limited mobilities in $Bi_{12}SiO_{20}$", P. Nouchi, J.P. Partanen, and R.W. Hellwarth, in Tecnical Digest on Photorefractive Materials, Effects, and Devices 1991, (Opt. Soc. Am., Washington, DC, 1991) vol. 14, pp. 236–239 (TuC10, Beverly, MA, July 29–31 1991).

4.115. "Spatial harmonics in photorefractive gratings, theory vs experiment", R.W. Hellwarth, Clarendon Laboratory, Oxford, England, 4 June 1991.

4.116. "Transport–induced–grating interferometry: application to photorefractive $Bi_{12}TiO_{20}$", Ping Xia, J.P. Partanen, and R.W. Hellwarth, in Tecnical Digest on Photorefractive Materials, Effects, and Devices 1991, (Opt. Soc. Am., Washington, DC, 1991) vol. 14, pp. 228–231 (TuC8, Beverly, MA, July 29–31 1991).

4.117. "Optical beam coupling by electron trap polarizability gratings in $Bi_{12}SiO_{20}$, Ping Xia, J.M.C. Jonathan, J.P. Partanen, and R.W. Hellwarth, paper CWD6 at the CLEO/QELS'91 Conference, Baltimore, MD, May 15 1991, Published in Conference on Lasers and Electro–Optics 1991, 1991 Tecnical Digest Series vol. 10, (Opt. Soc. Am., Washington, DC, 1991) pp. 236–237.

4.118. "Atoms for logic", R. Knize, B. Ai, D. Glassner, R.W. Hellwarth and J.P. Partanen, paper K1530 at the 1991 Annual Meeting of the Division of Atomic, Molecular and Optical Physics of the Am. Inst. of Phys., Washington, DC, April 24 1991, Abstract in Bulletin of the American Physical Soc., vol. 36, p. 1374 (1991).

4.119. "Atoms for logic", R.W. Hellwarth, Laboratoire de Physique des Lasers, Univ. of Paris–Nord, Villeteneuse, France, 25 June 1991.

4.120. "Atoms for logic", R.W. Hellwarth, Institut d'Optique, Orsay, France, 2 July 1991.

4.121. "Optical logic with single photons", R.W. Hellwarth, Bellcore Laboratories, Red Bank, New Jersey, 22 Oct 1991.

4.122. "Thinking about laser gravity wave detectors", R.W. Hellwarth, 6th Annual Theoretical Physics and Quantum Optics Summer Festival, Max–Planck Institut fur Quantenoptik (MPQ), Garching, Germany, 11 July 1991.

5. Advanced Degrees Awarded and Professional Personnel 12/1/90 to 11/30/91

5.1. "Four wave mixing in photorefractive and polymeric materials: ring phase conjugator and time–resolved measurement of third order optical nonlinearity," Jien–Ping Jiang, Ph.D. Thesis (Physics), USC, Dec. 1990.

Other professional personnel supported under this research project:

5.2. Dr. J.P. Partanen

5.3. Dr. J.M.C. Jonathan

5.4. Ms. Ping Xia

5.5. Ms. Pascale Nouchi

5.6. Mr. Patrick Tam

5.7. Mr. David Glassner

5.8. Mr. Nansheng Tang

6. Interactions 12/1/90 to 11/30/91

The interactions by members of this project are, in addition to the talks, conferences, workshops and seminars listed in Section 4, the consulting services performed by Professor Hellwarth for Lawrence Livermore National Laboratory (contact: Dr. Mark Henesian), for Los Alamos National Laboratory (contact: Dr. D.F. Dubois), and for the Hughes Research Laboratory (contact: Dr. C.R. Giuliano). The subject matter of this consultation was lasers and laser beam interactions.

7. Inventions

No invention disclosures were filed in this period.

Appendix I

SYNTHESIS AND CHARACTERIZATION OF THIRD ORDER NONLINEAR OPTICAL MATERIALS

L. P. YU*, M. CHEN* and L. R. DALTON*, X. F. CAO**, J. P. JIANG** and R. W. HELLWARTH**
*Department of Chemistry, University of Southern California, Los Angeles, CA-90089;
**Department of Electrical Engineering and Physics, University of Southern California, Los Angeles, CA-90089.

ABSTRACT

New polymers incorporating a variety of electroactive moeities with defined π-electron conjugation lengths have been synthesized and characterized by degenerate four wave mixing (DFWM) techniques. The $\chi^{(3)}/\alpha$ values for these materials varied from 10^{-12} to 10^{-13} esu cm. This work has identified several promising structures with nonlinear optical activity including organometallic and purely organic materials. The preparation of composite materials has also permitted the measurement of $\chi^{(3)}/\alpha$ as a function of the electroactive unit concentration.

INTRODUCTION

Nonlinear optical (NLO) properties of polymers is a rapidly growing research field because of the many practical applications of polymeric materials in optoelectronic devices.[1] Polyconjugated materials like polydiacetylene, polyacetylene and polythiophene have been heavily investigated.[1-3] But the inherent deficiencies of these materials, such as poor solubility, poor thermal and environmental stability and high optical absorption losses, prevent their use in practical applications. Therefore, new materials must be found. Both theory and experiment have demonstrated that polymers with limited conjugated length can manifest NLO effects as large as polymers with extended polyconjugation.[4-6] It has been recognized that electron delocalization and charge transfer contribute to NLO effects, and that polymers with electron clouds of enhanced anharmonicity are expected to give rise to large NLO effects. [3,7] Therefore, it is reasonable to test different materials with different kinds of constituents for optical nonlinearities. Such materials would include those containing transition metals and polymers with ionic or with charge separated

Abbreviations: Fourier Transform Infrared (FTIR), Nuclear Magnetic Resonance (NMR), Ultraviolet/visible (UV/vis), Gel Permeate Chromatography (GPC), Differential Scanning Caloriometer (DSC), Dimethylformamide (DMF), Dimethylsulfoxide (DMSO).

Mat. Res. Soc. Symp. Proc. Vol. 173. ©1990 Materials Research Society

species. With this in mind, we have extended our research to a broader survey of conjugated electroactive units. Here we report part of our effort in the synthesis and characterization of new materials exhibiting large optical nonlinearities.

EXPERIMENTAL

Polymer 1. This polymer was synthesized through a precursor polymer.[6] The mixture of prepolymer (0.904 g, 1.97 mmol) with nitrobenzene (20 mL) and benzoyl chloride (3 mL) was refluxed for 4 hrs. The reaction mixture was poured into methanol (50 mL) and the red precipitate was collected by filtration and washed with methanol until the filtrate becomes colorless, yielding polymer 1 (1.09 g, 83%). ^{1}H NMR (DMSO-d_6) d 1.6, (broadened, 6H), 3.9, (broadened, 4H), 6.5-8.2 (broadened, 18H) ppm.

Anal. Calcd for $(C_{37}H_{28}N_2Cl_2O_6)_n$: C, 66.56, H, 4.20, N, 4.20, Cl, 10.64%. Found: C, 66.12, H, 3.87, N, 3.75, Cl, 11.45%.

Polymer 2. The mixture of monomer (1,6-di(1-ethyl,2-methyl-quinolidine-6-oxy) pentane diiodide) (1.00g, 1.36 mmol) with triethyl orthofomate (0.739 g, 5.44 mmol) and pyridine (15 mL) was refluxed for one hr. The mixture was poured into THF. The precipitate was collected and washed with cold methanol. The final product was dried at 40°C under vacuum overnight, yielding polymer 2 (0.73g, 85%). ^{1}H NMR (DMSO-d_6) d 1.4, (t, J=9.0 Hz, CH_3- of ethyl), 1.8, (broadened, -$(CH_2)_3$-), 3.0, (s, overlapped with water side band, 2-methyl), 4.3, (broadened, -OCH_2-), 5.0 (broadened, -CH_2- of ethyl), 6.5 (broadened, =CH-), 7.0-9.0, (multiple, aromatic protons).

Anal. Calcd. for $(C_{119}H_{145}N_8O_8I_5)5H_2O$: C, 56.26, H, 6.11, N, 4.41%. Found: C, 56.43, H, 5.78, N, 4.40%.

Polymer 3. The mixture of monomer[11] (1.00 g) and AIBN (0.003g) was added to toluene (20 mL) in a tube. The solution was frozen and thawed twice under vacuum to remove oxygen and was then sealed. The sealed tube was immersed in a oil bath at 70°C overnight. The reaction solution was poured into ether and the polymer was collected by filtration and washed with ether. The product was then dried at room temperature under vacuum overnight, yielding polymer 3.(0.3 g, 30%).

Anal. Calcd. for $(C_{30}H_{32}N_4O_3)0.3H_2O$: C, 71.79, H, 6.50, N, 11.17%. Found: C, 71.94, H, 6.54, N, 11.22%.

Polymer 4. Squaric acid (0.91 g, 7.98 mmol) was dissolved in 20 mL hot butanol and then N-methylpyrrole (0.65 g, 7.98 mmol) was added. The mixture was refluxed for 2 hrs. The dark blue precipitate was collected and washed with water and ethanol, dried at 50°C under vacuum yielding polymer 4 (1.16, 80%).

Anal. Calcd. for $(C_{55}H_{40}N_7O_{10})5H_2O$: C, 63.03, H, 4.68, N, 9.36%. Found: C, 63.07, H, 4.87, N, 9.65%.

Polymer characterization and DFWM experiments have been described in previous works. [6, 12]

RESULTS AND DISCUSSION

The following materials (polymers and small molecules) have been synthesized and characterized by DFWM techniques (See Fig. 1).

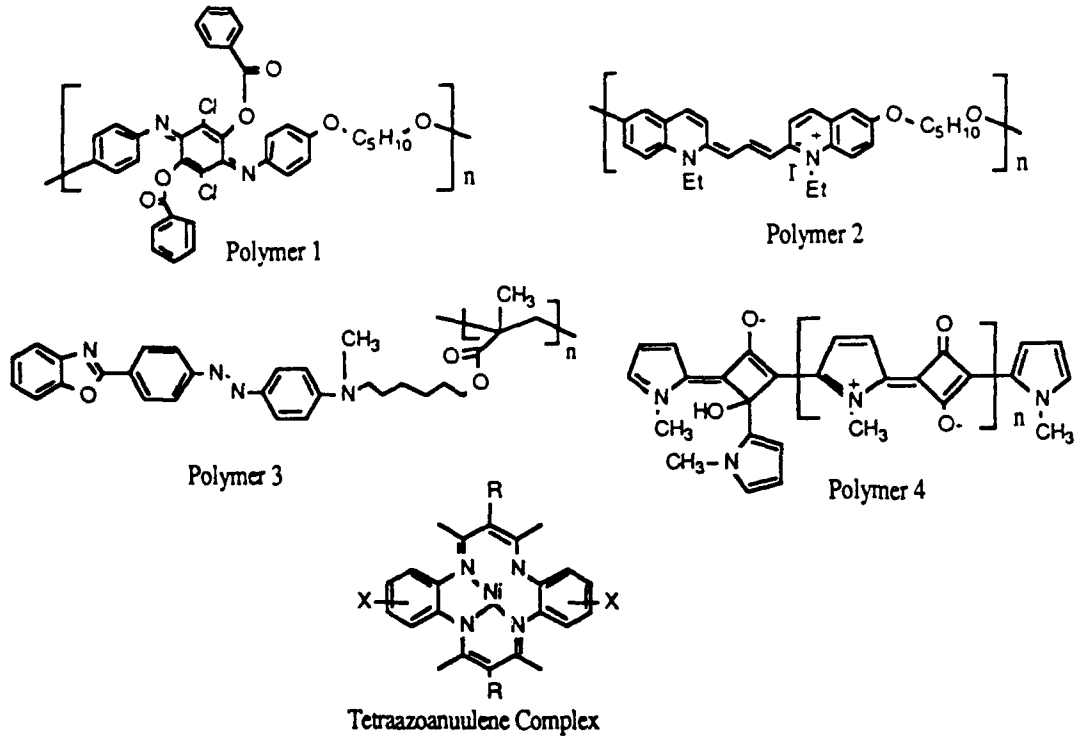

Fig. 1: Structures of NLO active materials.

Polymer 1 is synthesized following reaction scheme 1.

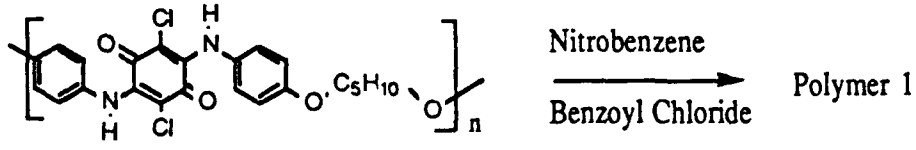

Scheme 1: Synthesis of polymer 1.

The polymer structure has been confirmed by FTIR, ^{1}H NMR, ^{13}C NMR, UV/vis spectroscopic studies and elemental analysis. Fig. 2a shows the Uv/vis spectrum of polymer 1. Sharp absorptions at ca. 479, 515 and 567nm can be found. Polymer 1 is fully soluble in DMF, DMSO and 1-chloronaphthene and optical quality films can be cast from these solutions. GPC measurements in DMF show that the weight average molecular weight, $<M_w>$, is about 20,000 using polystyrene as a standard. This polymer is thermally stable up to 480°C

Polymer 2 is synthesized through a well known cyanine dye formation reaction (see scheme 2).

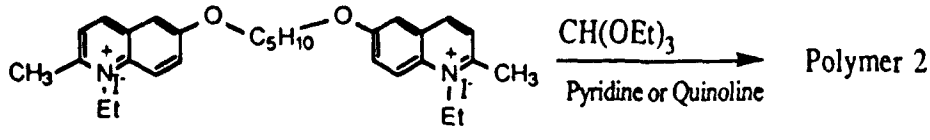

Both pyridine and quinoline can be used as solvents. Since these solvents are not good solvents for the final products, the materials we obtained are not high molecular weight polymers. Elemental analysis showed that they have only about three repeat units. They are partially soluble in DMF, DMSO and m-cresol. The films can be cast from solution or from mixed solution with polycarbonate on glass slides. ^{1}H NMR spectra shows that a broad peak at 6.5 ppm attributed to methine proton appears and the 2-methyl peak of the monomer decreased dramatically. FTIR spectra show similar features with those of model compound, 6,6'-dimethoxy-quinolidine cyanine. Fig. 2b shows the Uv/vis spectrum of polymer 2 in which absorptions appear at 540, 580 and 640 nm.

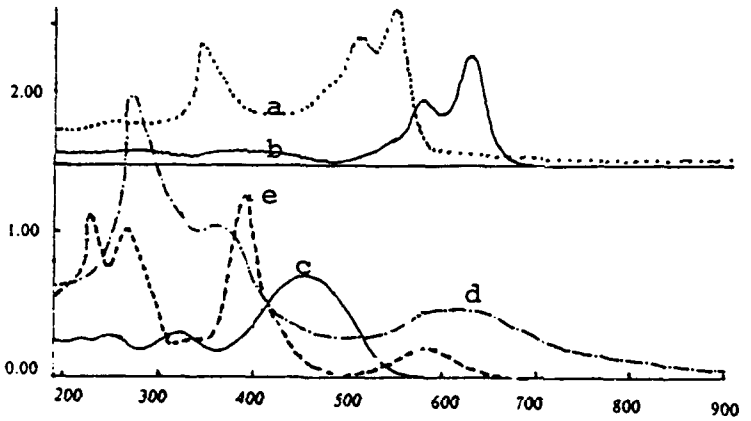

Fig. 2: Uv/vis spectra of a). Polymer 1, b). Polymer 2, c). Polymer 3, d). Polymer 4 and e). Tetraazoanuulene nickel complex.

Polymer 3 is synthesized by a free radical polymerization of the corresponding a-vinyl monomer.[11] The final polymer has MW of 4000 to 10000 (polystyrene as standard). ^{1}H NMR, ^{13}C NMR, FTIR, Uv/vis spectroscopic data and elemental analysis results confirm the structure proposed. Fig. 2c gives the Uv/vis spectrum of polymer 3. This polymer is thermally stable up to 300°C as shown by TGA studies. DSC shows T_g at 40°C and no liquid crystal transitions have been observed between 0°C-200°C.

Polymer 4 is a known polymer which was synthesized by Treibs and Jacob[8] with only three repeat units. We modified the synthesis procedure and obtained a polymer with a repeat units larger than five. The elemental analysis results suggest that each squaric acid unit is associated with one water molecule. TGA and DSC studies support this assumption. A weight loss of 7% accompanied by a endothermic process were observed between 50-140°C. It is partially soluble in DMF and m-cresol and forms blue solutions. FTIR spectra show absorption at 1775 cm^{-1}(s) due to the carbonyl group of the squaric acid unit, absorption at 1640 cm^{-1} (vs) due to the vinyl group in the squaric acid unit and methyl absorption is observed around 2890 cm^{-1}. Fig. 2d is the Uv/vis spectrum of this polymer in which the lowest absorption band appears around 610 nm. This polymer is very interesting because it can have many resonance structures in which the charge separated structure is the most likely one.[8]

Tetraazoannulene complexes are synthesized according to a known procedures.[9] We are interested in these compounds because they contain transition metals (Ni can be replaced by Cu and Fe etc.) and they are soluble in common organic solvents. They can be derivatized by different substitutents both at the R and X positions, which provide opportunity for incorporating them into polymer backbone. Fig. 2e shows the Uv/vis spectrum of compound with R=X=H, in which a window around 530 nm can been seen. This is an advantage for DFWM measurements, usually performed at 532 nm.

All these materials have been demonstrated NLO active by DFWM experiments. Table 1 summarized the results for these materials.

Table I. NLO properties of Polymers 1-4 and Tetraazoannulene Nickel complex.

Materials	$\chi^{(3)}/\alpha$ (esu. cm) x 10^{13} at l=532 nm
polymer 1	0.37
polymer 2	9.00*
polymer 2 in polycarbonate 10%	0.86
polymer 3	8.50*
polymer 4 in polycarbonate 10%	0.90
complex in polycarbonate 10%	2.45

* Permanent grating has been observed in high pulse energy.

Fig. 3 shows a typical plot of the DFWM signal pulse energy versus the delay time of the backward pump beam B for polymer 1. From Fig. 3, we can see an extremely fast NLO process at zero delay time, which might be attributed to an electronic excitation contribution, and a slower process which might arise from thermal contributions. Polymers 2 and 4 show similar signal patterns. It can be noted from Table I. that polymer 2 and polymer 4 have similar $\chi^{(3)}/\alpha$ values in polymer matrix which they are larger than polymer 1 and, in this case, might mean that the charge species and/or longer conjugation make significant contributions. The results in Table I are comparable with those of polyconjugated polymer systems such as polyacetylene and polythiophene. It demonstrates that high third order NLO effect can be observed in polymer systems with moderate conjugation lengths. In Table I, the $\chi^{(3)}/\alpha$ value for tetraazoanuulene nickel complex is very high and is comparable to those of phthalocyanine complexes.[10] We are now trying to incorporate this complex into a polymer backbone so that the processibility of the materials can be improved.

CONCLUSION

The processibilities of NLO polymers can be improved by introduction of flexible chain to link electroactive unit. The polymers so obtained with moderate conjugation lengths can manifest optical nonlinearities as large as polymers with extended polyconjugations.

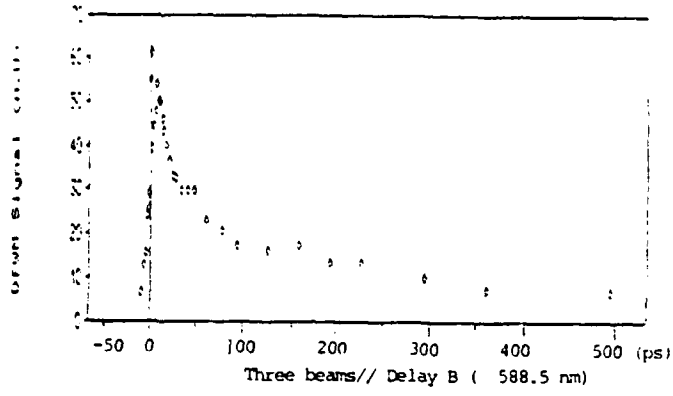

Fig. 3: Plot of DFWM signal as a function of delay time.

ACKNOWLEDGEMENTS.

This work was supported by Air Force Office of Scientific Research contracts F49620-87-C-0100 and F49620-88-C-0071 and by National Science Foundation grant DMR-88-15508.

REFERENCES

1. A. J. Heeger, J. Orenstein and D. R. Ulrich. Eds. Nonlinear Optical Properties of Polymers. Symposium Proceedings; Materials Research Society, 1989, vol. 109.
2. L. Yang, R. Dorsiville, Q. Z. Wang,W. K. Zou, P. P. Ho, N. L. Yang R. R. Alfano, R. Zamboni, R. Danieli, G. Ruani, and C. Taliani. J. Opt. Soc. Amer. B 1989, vol. 6, 753.
3. S. A. Jenekhe, S. K. Lo, and S. R. Flom. Appl. Phys. Lett. 1989, 54, 2524.
4. C. P. de Melo and R. Silby. Chem. Phys. Lett. 1988, 140, 537.
5. J. R. Heflin, K. Y. Wong, O. Z. Khamir and A. F. Garito. Phys. Rev., 1988, B38 1573.
6. L. P. Yu and L. R. Dalton. J. Amer. Chem. Soc., 1989, 111, 8699.
7. P. N. Prassad, E. Perrin and M. Samoc. J. Chem. Phys., 1989, 91, 2360.
8. A. Treibs and K. Jacob. Liebigs Ann. Chem., 1966, 699, 153.
9. D. A. Place, G. P. Ferrara, J. J. Harland and J. C. Dabrowiak. J. Heterocyclic . Chem. 1980, 17, 439.
10. L. P. Yu, R. Vac, L. R. Dalton and R. W. Hellwarth. SPIE proceedings, 1989, vol. 1147.
11. M. Chen, L. P. Yu and L. R. Dalton. (in preparation).
12. X. F. Cao, J. P. Jiang, D. P. Bloch, R. W. Hellwarth, L. P. Yu, and L. R. Dalton. J. Appl. Phys., 1989, 65, 5012.

Appendix II

PROCEEDINGS REPRINT

SPIE—The International Society for Optical Engineering

Reprinted from

Nonlinear Optical Properties of Organic Materials III

11-13 July 1990
San Diego, California

Volume 1337

Bipolaronic Enhanced Third Order Nonlinearity in Organic Ladder Polymers

X.F. Cao, J.P. Jiang , R.W. Hellwarth

Department of Electrical Engineering and Physics

L.P. Yu, M. Chen, L. Dalton

Department of Chemistry

University of Southern California
Los Angeles, CA 90089-0484

ABSTRACT

Third order nonlinear optical properties of organic ladder copolymer (POL) system is studied using degenerate four-wave mixing with picosecond laser pulse. Both the real and imaginary part of the third order nonlinear susceptibility $\chi^{(3)}$ were determined by a new phase conjugate interferometric method over the wavelength range of 532 - 720 nm. From the space symmetry and wavelength dependence of $\chi^{(3)}$ we attribute the observed nonlinearity to the nonlinear photoexcitation of bipolarion states in this ladder copolymer system.

1. INTRODUCTION

Although it is recognized that delocalized pi-electron polymers exhibit large nonlinear optical response, of particular interest is their capability of exhibiting *fast nonresonant* $\chi^{(3)}$ *values* for potential all-optical device application.[1] However, several practical problems have limited the further exploitation of these nonlinear optical properties. One of the major difficulty is to find large optical nonlinearity with small optical absorption. True non-resonant nonlinearity is not expect to be large. Another avenue for exploiting large nonresonant nonlinearity is to look for subgap resonant processes with small one photon absorption. Unfortunately for subgap resonant process such as two-photon absorption, the dominant contribution of the optical nonlinearity comes from nonlinear absorption. [2] It has been recently pointed out that nonlinear absorption can also induced the undesired thermal effects under intense irradiations just as in the case of linear absorption. [3] In order to ultilize the advantage of the fast reponse nonllinearity in organic materials, it seems that efforts should be concentrate on looking for large, real, subgap resonant, fast response optical nonlinearity in organic materials.

Ladder polymers have excellent chemical and thermal stabilities and have recently been shown that stable bipolarion state s can be induced in model ladder structure related to PTL and POL systems.[4] It is shown by electron nuclear double resonance (ENDOR) and electron spin echo (ESE) spectroscopies, that electron delocalization might not extended much beyond one ladder repeat unit. In the view of the fact that the polarionic electron delocalization in ladder polymers may in fact be confined to an average of one repeat unit,[5] it seemed appropriate to study the possibility of formation of the less-confined bipolarionic states in ladder model systems such as POL structure illustrated in Figure 1.

Experimental results of electro-chemical doping have indicated the bipolarion state is the more stable state and can easily be achieved with excess dopant. In addition, electron-donating groups stabilized the bipolarionic state significantly. Bipolarion states generated by electro-chemical doping in monomer PTL ladder model system has been shown to be stable in the presence of moist air for several days.[4]

In this paper , we study the possibility of photoexcitation of bipolarions in POL model ladder system by investigating optical nonlinearity in this system. Both the real and imaginary part of the third order nonlinearity is determined by using a modified phase conjugate interferometric method over the wavelength range of 532 - 720 nm. comparison between the nonlinear photoexcitation of bipolarons and the bipolarions generated by electro-chemical doping will be discussed.

2. EXPERIMENT AND RESULTS

Among different experimental methods in studies of third order nonlinear optical properties of materials, degenerate four-wave mixing is the most sensitive one. Extreme small index change ($\Delta n = 10^{-6}$) can be detected easily by this method. However this method is only sensitive to the magnitude of the complex third order nonlinear susceptibilities $\chi^{(3)}$, the phase of $\chi^{(3)}$ cannot be detected by this method. In this section we described a new interferometric method which can determined the real and imaginary part of $\chi^{(3)}$ $(-\omega, \omega, \omega, -\omega)$ accurately at the same time. This technique was first proposed by Rentzepis et.al. [6] In this study we have extended this technique to the picosecond pulse measurement in nonlinear thin films.

This interferometric method is base on a modified Twyman-Green interferometer, which includes two phase conjugate mirrors. As will be discussed in the following , this interferometer makes possible the accurate measurement of relative phase shift between two phase conjugators. A schematic representation of this double phase conjugate interferometer is shown in Figure 2, two phase conjugate mirrors are based on degenerate four-wave mixing scheme. The forward pump beam and probe beam are split into two sets by a beam splitter BS, and follow the two paths shown in Figure 2. The backward pump beams are provided by the back reflections of the forward pump beams from the mirrors right next to the two nonlinear samples. After interacting at the phase conjugate mirror, phase conjugate beams PC1 and PC2, and two retroreflected backward backward pump beams recombine at BS. Such a setup consists two Twyman-Green interferometers, two backward pump beams interfere with each other forms a conventional interferometer which we designate it as pump interferometer PI. The two phase conjugate beams constitute a phase-conjugate interferometer CI. The alignment of one interferometer, PI or CI, results in automatic alignment of the other. In the experiment , the alignment of PI is achieved by eliminating the the interference fringes in front of the detector PD1, perfect alignment is reach when a circular ring pattern is found. The center spot of this circular pattern is selected by a pinhole and then sent to the detector. A piezoelectric transducer, PZT is mount on the back of the high reflector in one arm to vary the path length difference between two arms. Also path difference between two arms must be roughly the same in order to temporal overlap two picosecond interference pulses. (In our case pulse length is about 6mm)

The best way to understand the data from this modified phase conjugate interferometers is to introduce a variable phase shift $\Delta\varphi$ into one of the arms of the interferometer and analyze how the interference pattern change with this phase shift. This variable phase shift can be introduced by moving one of the backreflection mirrors behind the nonlinear sample. The interference signal of the pump interferometer, I_{PI} is

$$I_{PI} = I_1 + I_2 - 2(I_1 I_2)^{1/2} \cos[4\pi(l_1 - l_2)/\lambda + \Delta\varphi], \quad (1)$$

where I_1 and I_2 are the intensities of the returning pump beams that follow the optical path lengths $2l_1$ and $2l_2$ of arms 1 and 2, respectively. Using the expression for phase conjugate signal, it is easy to show that the interference signal I_{CI} of the phase conjugate interferometer CI can be written as

$$I_{CI} = I_{C1} + I_{C2} - 2(I_{C1} I_{C2})^{1/2} \cos[4\pi(l_1 - l_2)/\lambda + \Delta\varphi + \varphi_{01} - \varphi_{02}]. \quad (2)$$

where φ_{01} and φ_{02} are absolute phase shifts of the phase conjugators, which depend on the type of diffraction grating created by the pump and probe beams. Comparison of equations (1) and (2) shows that the interference signals at two outputs are described by the same function of the induced phase shift $\Delta\varphi$. The only difference is the phase shift $\varphi_{01} - \varphi_{02}$. This phase shift is equal to the difference of absolute phase of $\chi^{(3)}$ $(-\omega, \omega, \omega, -\omega)$ in the two nonlinear mediums. This means that, if the absolute phase shift in one of the nonlinear material is known, then the absolute phase of other materials can be determined easily. In the case when same medium is used in both arms, the interference signal at both outputs should be exactly in phase. Also the ration between the maximum and minimum of the interference pattern can be used to determine the ratio of $\chi^{(3)}$ $(-\omega, \omega, \omega, -\omega)$ in both mediums accurately.

To determine the absolute phase of in POL ladder copolymer system, experiments using this interferometer have been performed over the wavelength range of 532 - 720 nm. To check the interferometer setup we initially used CS_2 in both interferometer arms. Two 1mm thick cells filled with CS_2 were placed in two arms. In the Figure 3, the interference signal of both CI and PI are plotted as a function of the PZT voltage. These data shows two signals are exactly in phase. ($\varphi_{01} - \varphi_{02} = \pm 3^{o}$) Next we put POL ladder copolymer thin films in one arm, and CS_2 cell in the other. CS_2 is transparent over this wavelength range, and it is well understood that its nonlinearity is mostly real and positive. Experimental results at 590 nm are shown in Figure 4, from this figure we found two interference signals are shifted by 114 ± 3^{o} , this suggests that $\chi^{(3)}$ $(-\omega, \omega, \omega, -\omega)$ of POL copolymer at 590 nm is mostly imaginary, and have a negative real part.

To determine the magnitude of the complex $\chi^{(3)}$ $(-\omega, \omega, \omega, -\omega)$, we have performed the traditional four-wave mixing experiment in POL ladder copolymer system. In this case, the backward pump beams is provided by a third laser pulse instead of using the reflection from the mirrors. *Knowing the magnitude and the phase of* $\chi^{(3)}$ $(-\omega, \omega, \omega, -\omega)$, we can determine its real and imaginary part at the same time. Also, by this setup, we are able to time delay pulse of different beams to study the transient dynamics of the photoexcited bipolarionic states. A typical decay data for phase conjugate signal as a function backward pump beam delay is shown in Figure 5.

We also study the tensor symmetry of the $\chi^{(3)}_{ijkl}$ $(-\omega, \omega, \omega, -\omega)$ by studying the polarization dependence of the phase conjugate signal. In the case when the probe beam polarization is vertical while the pump beam polarizations are horizontal, phase conjugation signal is at least 1000 times smaller than in the case when all beam polarization are horizontal. This result indicates that $\chi^{(3)}_{1221} < \chi^{(3)}_{1111}/30$, therefore suggest that the observed nonlinearity is relate to a nonlinear population excitation.

3. DISCUSSION

In order to understand the the photogeneration bipolaron process, we will first discuss some feature of bipolaron generation by electro-chemical doping. In essence , during the doping process, a new subgap band structure which is shifted far to the red , replace the original π-π^* band of the POL compounds. There are three significant signatures of the generation of bipolarionic states: (1) The formation of localized structural distortions with associated localized vibrational modes (IRAV modes) in the midinfrared. (2) The generation of symmetric gap states and the associated electronic transitions. (3) The reversed spin-charge relation, i.e., charge storage in *spinless* bipolarons.

In POL ladder system all these features have been verified experimentally during electro-chemical doping. Absorption spectra change due to doping indicates the formation of subgap states. [4] We have also performed electron spin resonance spectroscopy (ESR) experiment for the doped and undoped samples, no ESR signal was observed under the saturate doping case. All these results in doped POL systems are in consistent with the picture of bipolarons generation.

Next we discuss the process of photoexcitation of bipolaronic state. The direct photogeneration of charge bipolaron is clearly impossible. After electron-hole photoinjection, the confinement resulting from the nondegenrate ground state will lead to rapid formation of a neutral "bipolaron", i.e., a neutral exciton with one electron in the lower gap state and one electron in the upper state. Such neutral "bipolarons" can be expected to undergo rapid radiative decay. This probably is the dominant mechanism at earlier times. Because of the transverse bandwidth due to interchain coupling, some of the initial photoexcitations occurs as electron and holes on different chains. Chain distortions will quickly form around these single charges, leading to polaron formation. Bipolarons can then be generated if energetically favorable.

From the results of our studies of optical nonlinearity, first of all, the tensor symmetry ($\chi^{(3)}_{1221} < \chi^{(3)}_{1111}/30$) of the observed nonlinearity indicated that the nonlinear mechanism is relate to photoinduced population of certain "excitons". This symmetry holds for all the wavelength we studied.

In Figure 6 , we plot the real and imaginary part of the $\chi^{(3)}(-\omega, \omega, \omega, -\omega) / \alpha$ as a function of wavelength. The solid curve is deduced from the absorption spectra change during the doping. By expressing the results this way, we have normalized the observed nonlinearity to the photoinduced change of optical properties (refractive index or absorption) per photon absorbed by the POL ladder copolymer thin films. This quantities is independent of the POL molecular density in the sample and can be compare with other sample with different POL concentration or even monomer unit mixed in polymer matrix. As seen in this figure , the imaginary part of the nonlinearity , or in other word , the photoinduced absorption, agrees well with the wavelength dependence of the absorption change due to electro-chemical doping. This indicates the photoinduced absorption spectrum is similar to the doping-induced absorption spectrum, therefore indicates the photogeneration of bipolaronic state in POL ladder copolymers.

We have also compared the results of copolymer and dilute monomer solid solution, in the case of monomer solution, about 3 times smaller $\chi^{(3)}(-\omega, \omega, \omega, -\omega) / \alpha$ value is found. This indicates the contribution of interchain coupling in the high density copolymer structure. However, 5 times higher optical damage threshold ($2GW/cm^2$ for 5 psec pulse) was found in the monomer solid solution (0.5% mol/mol). Even in this dilute concentration of POL units , no evidence of polaron generation is observed.

Transient decay dynamics of the photogeneration of bipolarons is studied by the picosecond resolved (5 psec resolution) degenerate four-wave mixing experiment. As seen form Figure 5, two decay processes is evident. A pump intensity dependent fast decay ($\tau = 8 \pm 2$ psec at intensity of 0.2 GW/cm^2), and an intensity independent slow decay ($t = 120 \pm 5$ psec). The intensity dependent fast decay characterized the rapid recombination of the neutral bipolarons. The slow decay process may be relate to interaction of defects in the structure. Same type of delay behavior was observed when the forward pump pulse was delayed. This result indicate s that the decay processes are local interaction coupling.

The significance of this observation is underlined by the fact that effective photogeneration of bipolaronic states can be achieved in short conjugated ladder systems such as POL. Our results indicate the possibility of obtaining large subgap resonant "bipolaron enhanced $\chi^{(3)}$ value in one repeat unit of ladder polymer structure. And as seen in Figure 6 , unlike two photon absorption , large real contribution of subgap resonant nonlinearity can be obtain at certain wavelength windows.

Because of the fact that effective nonlinear excitation process can be support in short ladder segments, we are able to observed high nonlinear optical activity in copolymer structures. The advantage of using copolymer structure is the nonactive spacer improved the solubility of the polymer. Thus processibility is attained while achieving a controllable optical widow and high nonlinear optical activity. We are currently exploring options of controlling optical windows, film forming characteristic and thermal properties of different ladder copolymer systems.

4. CONCLUSION

In summary, we have observed the first experiment evidence of photogeneration of bipolaronic states in organic ladder copolymer systems. The photoinduced absorption spectrums is similar to the doping- induced absorption spectrums. Large, supgap resonant, real, fast response optical nonlinearity together with good thin film processibility and stability can be achieved in these copolymer systems.

5. ACKNOWLEDGEMENTS

This work was supported by AIR Force Office of Scientific Research contracts F 49620-88-C-0071 and grant #EET-8513857.

6.REFERENCES

[1] "Nonlinear Optical and Electroactive Polymers", P.N. Prasad and D.R. Ulrich, Eds., Plenum Press, New York, 1988.

[2] M. Lequime and J.P. Hermann, Chem. Phys. 26, 431 (1977).

[3] E. Caglioti, S. Trillo, S. Wabnitz, and G.I. Stegeman, J. Opt. Soc.Am. B5, 472, (1988)

[4] C.W. Spangler, T.J. Hall, K.O. Havelka, M. Badr, M.R., McLean and L. Dalton, SPIE proceeding 1147, paper16. 1989.

[5] L.R. Dalton, J. Thomson, and H.S. Nalwa, Polymer, 28, 543, (1987).

[6] S. M. Saltiel, B. Van Wonterghem and P.M. Rentzepis, Opt. Lett. 14, 183, (1989)

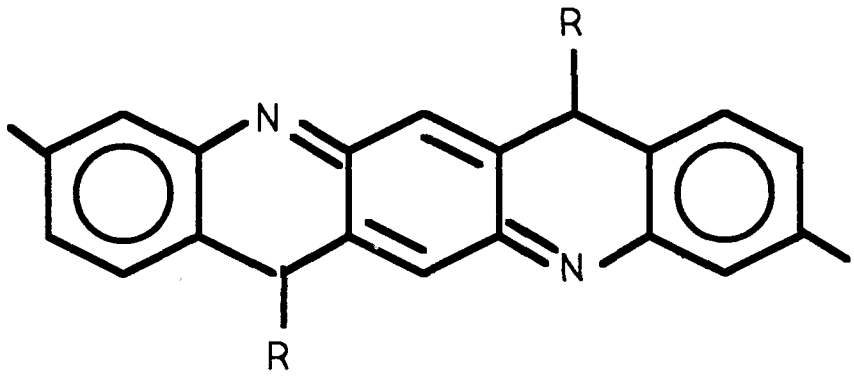

Fig. 1 Chemical structure of POL ladder monomer 1.

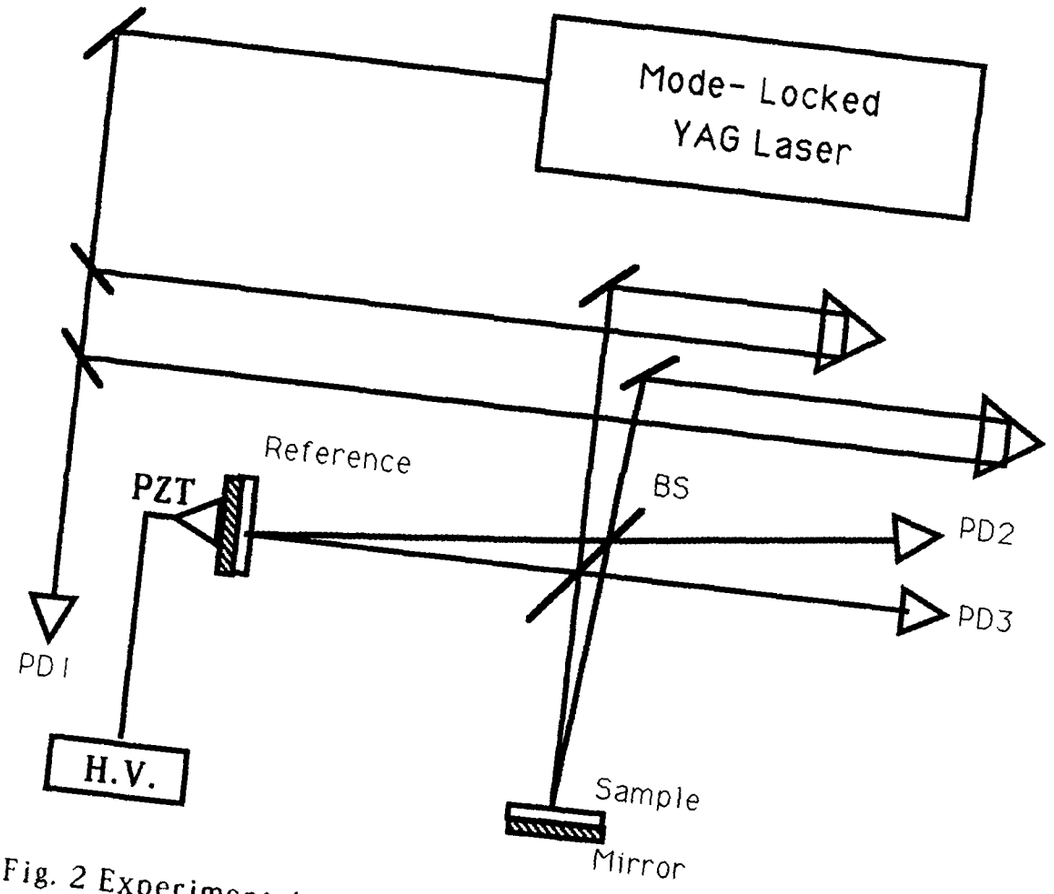

Fig. 2 Experimental setup of the double phase-conjugate interferometer.

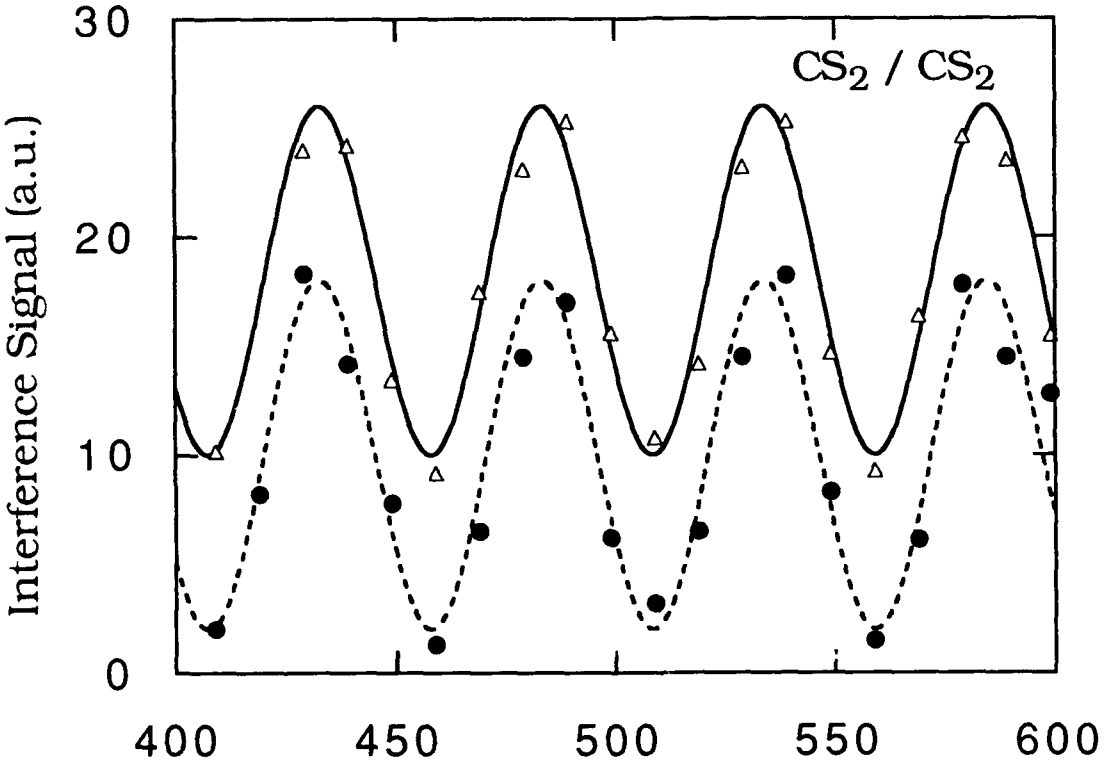

Fig. 3 Interference patterns of the pump interferometer (--●--) and phase conjugate interferometer (--Δ--)

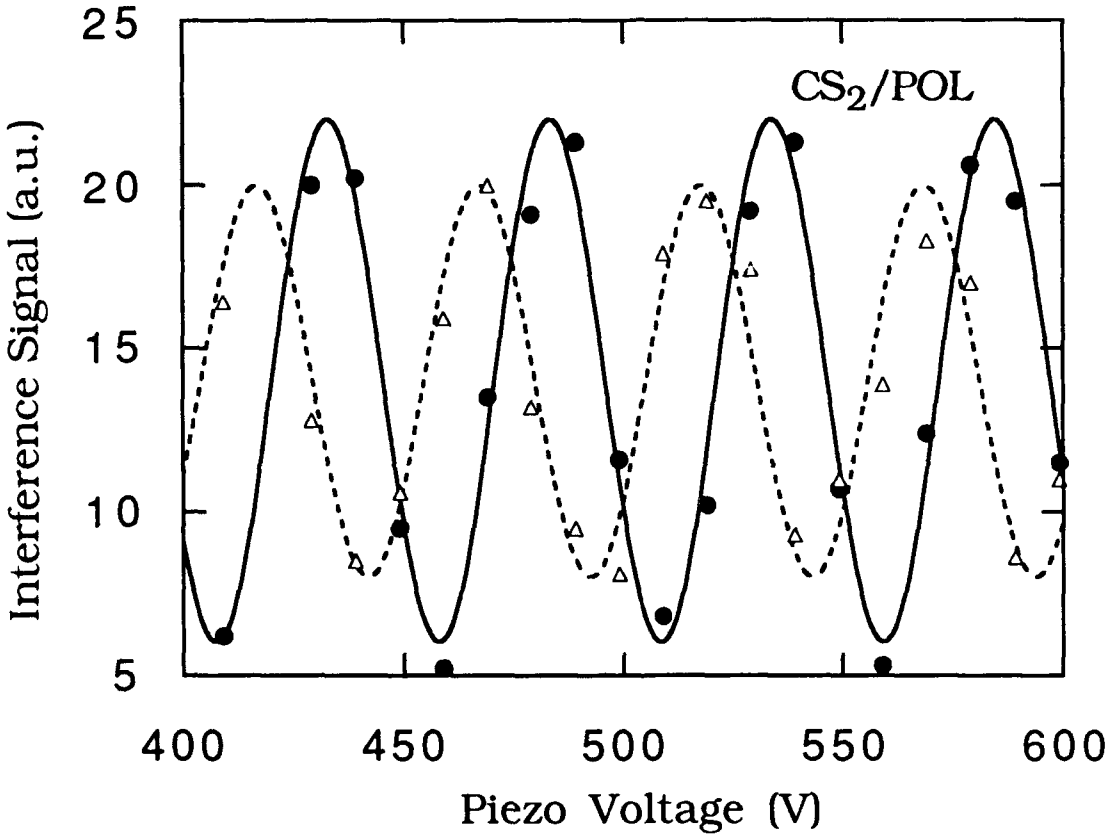

Fig. 4 Interference patterns of the pump interferometer (--●--) and the phase conjugate interferometer (--Δ--).

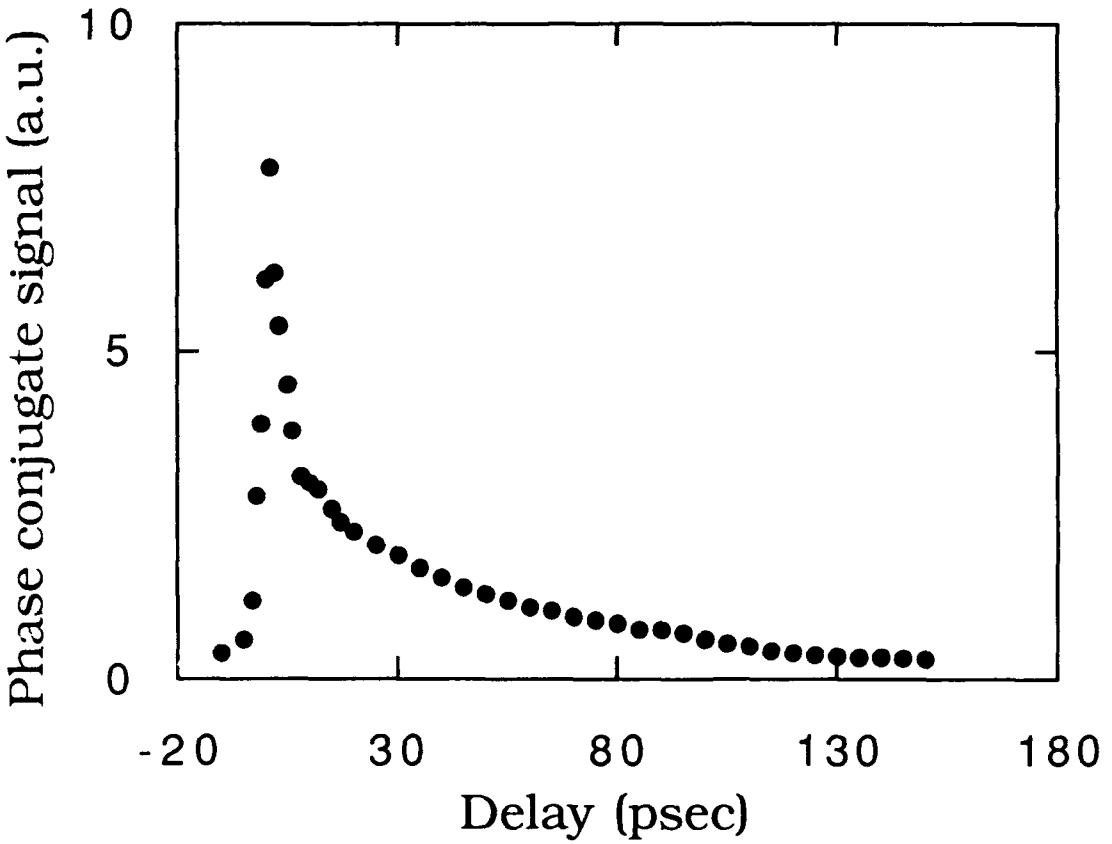

Fig. 5 Phase conjugate signal as a function of the delay of backward pump pulse.

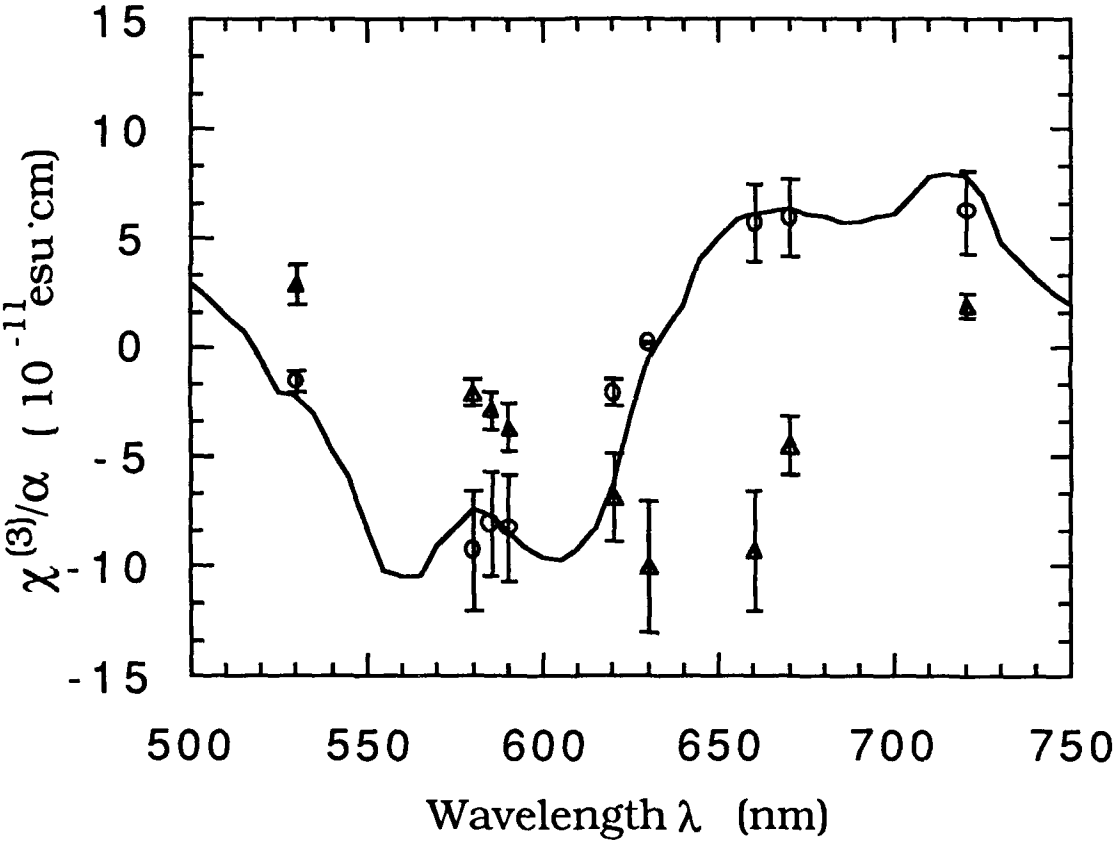

Fig. 6 Wavelength dependence of the real (---Δ---) and imaginary (---o---) part of $\chi^{(3)}$ (-ω, ω, ω, -ω) / α in POL ladder copolymer 1. The solid line is the normalized absorption spectra change during electro-chemical doping.

Appendix III

PHYSICAL REVIEW B VOLUME 43, NUMBER 16 1 JUNE 1991

Anomalous optical transmission in homogeneous latex suspensions

Patrick W. Tam and R. W. Hellwarth
Departments of Physics and Electrical Engineering, University of Southern California, Los Angeles, California 90089-0484
(Received 15 October 1990)

We have observed a deviation from the law of exponential attenuation of a 633-nm optical beam in a homogeneous scattering medium in the low-intensity limit, where nonlinear optical effects or thermal effects are insignificant (Bouguer's law). This deviation occurs when the spatial correlation length is comparable to or larger than the asymptotic attenuation length, whence the assumption of independent scattering events is violated. We develop a statistical model for the optical dielectric fluctuations which fits well our nonexponential beam-transmission data in homogeneous suspensions of 1-μm latex spheres. We use this to determine the correlation lengths (7 to 12 μm) of the dielectric fluctuations in these suspensions. These correlation lengths are consistent with values that we deduce from the observed angular spreads of forward light scattering.

I. INTRODUCTION

In 1729 Pierre Bouguer proposed that "in a medium of uniform transparency the light remaining in a collimated beam is an exponential function of the length of its path in the medium,"[1] an idea which was popularized by J. H. Lambert thirty years later. Here we report an observed exception to this law of exponential attenuation for low-intensity light beams. We study liquid suspensions in which the attenuation length ($\simeq 1$–3 μm) is of the same order of magnitude as the correlation length ($\simeq 7$–12 μm) of the fluctuations of the optical dielectric constant, thus violating the usual assumption (stated explicitly by Bouguer) that events which attenuate the beam are uncorrelated. We measure the relation between the optical transmission T through latex suspensions (polystyrene spheres in water) and their thickness L for five concentrations of the same particle size for which the transmission does not scale exponentially with the thickness. Optical transmission in latex suspensions has been studied by Ishimaru and Kuga, who studied the relation between the transmitted beam fraction T of samples of latex suspensions and the latex particle density.[2] They observed exponential decays of transmission T with thickness L, but the attenuation coefficient was not proportional to particle density N at the higher densities. That is, "Beer's law" was violated, a fact with which our results will correlate. The error in attenuation measurements arising from scattered light in latex suspensions at low concentrations ($<0.27\%$) was studied by Zaccanti and Bruscaglioni.[3] This error our method will avoid. In this paper, we describe an experimental technique that is sensitive to nonexponential transmission, and then develop a Gaussian statistical model for dielectric fluctuations which fits well the nonexponential attenuation we observe. We determine the spatial correlation-length parameter L_c in this model which gives the best fit to the data using two different forms for a correlation function. These forms give L_c values which agree within 20% with each other and with the correlation length estimated from the angular spectrum of the forward singly-scattered light. We describe numerous checks of possible extraneous influences and find these negligible. Our correlation-length measurements suggest the existence of long-range forces.

II. MEASUREMENT OF BEAM TRANSMISSION

We use as scattering material colloidal suspensions of monodisperse latex (i.e., polystyrene) spheres of diameter 1.09 ± 0.03 μm as specified by Sigma Chemical Company. As purchased, the volume fraction is approximately 10% which corresponds to a number density $N=1.48\times10^{11}$ cm^{-3}, and a nearest-neighbor separation of 1.9 μm (assuming a simple cubic lattice), which is about twice the diameter of the particles. Using a pH meter[4] we measured this sample to have a pH of 6.6 ± 0.3. We measured the dc conductivity to be $(7.3\pm0.5)\times10^{-4}\Omega^{-1}$ m^{-1}. More dilute samples are prepared by adding deionized water. More concentrated samples are prepared by letting the suspension settle and decanting the water. The samples are homogenized in an ultrasonic bath for several minutes, after which they remain stable for more than a half day, adequate time for a complete set of data to be obtained.

We have devised an experimental technique for determining beam transmission T vs sample thickness L that employs a direct comparison with the transmission through a variable-length cell containing a dye of known transmission function. This comparison is essentially a null comparison that keeps all detector signals within a small range. The experimental setup is described in Fig. 1. The variable-thickness spectrometer cell $C1$ contains the latex suspension while the standard comparison cell $C2$ contains a calibrated dye solution (Nile Blue in methanol).[5] A He-Ne laser emits a vertically polarized 10 mW, 633 nm $TEM_{(x)}$ Gaussian beam of radius 0.7 mm at $1/e^2$ intensity whose attenuation in the cells is studied

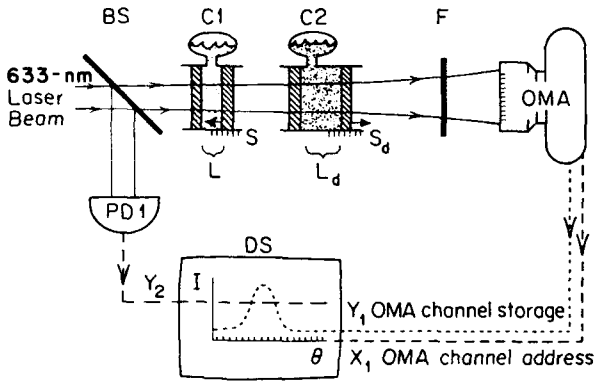

FIG. 1. Experimental setup for the measurement of optical transmission. Beam splitter BS and photodiode PD1 monitor the power incident on the variable-length cell $C1$ containing the latex suspension. The compensating variable attenuator $C2$ (containing dye solution) keeps the transmitted beam power into the (500 channel) optical multichannel analyzer OMA nearly constant. Filter F blocks fluorescence from the dye. Data is analyzed by digital oscilloscope DS.

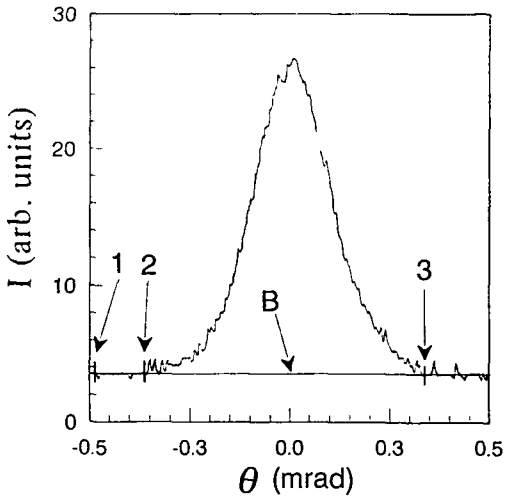

FIG. 2. A typical trace of beam intensity I vs angle θ from beam axis as measured by the OMA. The background B of scattered intensity is approximately constant in this small angular range and is computed by averaging the intensity from point 1 to 2. The area A under the Gaussian curve, with the background B as the baseline, is computed by a processor in the oscilloscope and used to calculate the beam fraction T transmitted through the suspension, as described in the text and plotted in Fig. 3. This trace is that used to obtain the data point marked P on trace B in Fig. 3. All other data points showed the same beam shape and width.

as follows. A small fraction of this beam is reflected off a beam splitter BS to a monitoring photodiode PD1, the output Y_2 from which is displayed on the digital oscilloscope DS. The other part of the beam traverses cells $C1$ and $C2$, after which the beam (of power ~ 10 nW) is detected by an optical multichannel analyzer OMA placed two meters beyond the latex sample.[6] The OMA measures the intensity profile of the transmitted beam at angles θ to the beam axis up to several beam widths. The OMA is shielded from fluorescence by interference filter F. The signal Y_1 from the OMA is averaged for 25 seconds and then stored in the digital oscilloscope DS as the intensity I opposite its address X_1 (which is a measure of the angular deviation θ from beam axis). A typical stored trace is shown in Fig. 2 which shows the transmitted Gaussian beam superposed on the background B of scattered light. Here, as in all of our transmitted beam profile measurements, we could never see any deviation of the beam shape or width from that which we observed with the cell $C1$ absent.

By rotating the threaded outer shell of the cell $C1$, we translate one of its glass windows through a distance given by the difference between two micrometer readings (correct to within ± 0.25 μm) on the outer shell which are indicated by S in Fig. 1. We express the relation between the scale reading S on $C1$ and the actual thickness L of the suspension by $S = L + L_0$, where L_0 is the scale reading corresponding to zero thickness. To avoid backlash problems, we take data by decreasing the thickness L of $C1$, while increasing the thickness L_d of $C2$ (with corresponding scale reading $S_d = L_d + L_{d0}$) to keep the peak signal at the OMA center channel constant to within 30%. This reduces the error in the measurements due to the nonlinear response of the detector to less than 1%. We start from the thickness of the suspension in $C1$ where we can detect a transmitted signal and reduce L to the thickness where the transmission levels off with further rotation of the outer shell. After each adjustment of the thickness L, the suspension is allowed to stabilize for several minutes before the measurement is performed. This is required to achieve reproducible data. At each of the scale settings S and S_d, a processor in the oscilloscope computes the average background intensity B using the formula $B = \sum I(\theta)/$(number of points sampled). Here the summation is taken from the point 1 to 2 as shown in Fig. 2. The area $A(S)$ under the Gaussian beam profile is then computed by $A(S) = \sum'[I(\theta) - B]$ where the summation $\sum'$ is taken from point 2 to 3.

We calibrate the dye solution by putting it in cell $C2$ with $C1$ removed. A photodiode is used instead of the OMA and the transmitted power is measured as the thickness of $C2$ is decreased, with calibrated neutral density filters placed in front of the detector when necessary. The transmitted power obeys Bouguer's law with an absorption constant $\alpha_d = 0.501 \pm 0.001$ mm^{-1} calculated by a least-squares fitting. To determine the transmission of the suspension $T(S)$ from S_d and $A(S)$ it is necessary to measure the absolute value of this transmission at some reference scale reading. Therefore, at the end of each set of measurements for a particular particle density, we determine the transmission $T(S_m)$ at the minimum scale reading S_m attainable (with corresponding scale reading S_{dm} on cell $C2$) by removing the cell $C2$ and measuring the transmitted beam power $P(S_m)$ with a silicon detector (here the transmitted power is too high for the OMA).

The cell $C1$ is then removed and the incident beam power P_0 measured with the same detector. Taking into account 4.5% reflection loss R from the window (4.2% from the glass-air interface and 0.3% from the glass-fluid interface), we calculate the transmission using $T(S_m)=P(S_m)/[P_0(1-R)^2]$. From this we get the transmission at other scale readings, to within 4%, by the relation $T(S)=T(S_m)A(S)\exp[\alpha_d(S_{dm}-S_d)]/A(S_m)$. At the end of the experiment on a given suspension the sample is weighed. After being dried in a vacuum oven for a day, the dried polystyrene is weighed again to determine the weight fraction of the polystyrene spheres. Using the density of a single latex sphere of 1.05 g cm^{-3} quoted by Sigma Chemical Company, we calculate the particle number density N of each sample to within an estimated uncertainty of less than 13%. The results of this procedure for five densities large enough to show deviations from Bouguer's law are shown in Fig. 3. The deviation from exponential behavior is most evident for the higher densities. The lines in Fig. 3 are the best fit to an equation which we derive using a phenomenological model for the statistics of the spatial distribution of the spheres. This equation fits the data to within experimental error for parameters which we describe in the next section. Since the cell has to be disassembled for cleaning after each set of measurements, the scale reading changes from one set of measurements to another by a small amount. The scale reading L_0 at zero thickness, which changes from one set of data to the other, is treated as a fitting parameter in the model which we now develop.

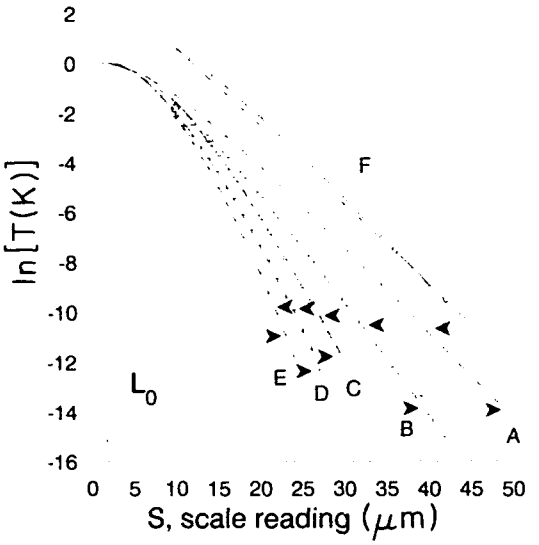

FIG. 3. Natural logarithm of the transmission T vs scale reading S (on $C1$) for five concentrations of the latex suspension. The particle diameter is 1.09 μm and the concentrations are given in Table I. The transmission is defined as the fraction of power remaining in the Gaussian beam (less background) after it traverses the latex suspension, and is calculated as explained in the text. Solid lines are a best fit according to Eq. (6) with the scale reading L_0 corresponding to zero thickness being an adjustable parameter. The values of the parameters are given in Table I. Curves F are typical limiting curves with off-center parameters used to determine the error bounds given in Table I; the data points are those of curve A shifted up by two units; the curve F is a plot of Eq. (6) with $\alpha_x=0.36\ \mu\text{m}^{-1}$, $L_c=11\ \mu$m, $L_0=-0.8\ \mu$m and $\alpha_x=0.32\ \mu\text{m}^{-1}$, $L_c=3\ \mu$m, $L_0=3\ \mu$m. The point P was obtained from the typical OMA trace shown in Fig. 2. The left-pointing arrows indicate the points where the beam size corrections estimated in the text are 100%. The right-pointing arrows indicate the points where the background intensities B are half of the corresponding peak intensities.

III. THEORETICAL MODEL FOR BEAM TRANSMISSION

We assume that a Gaussian beam propagates along the z axis and enters a turbid medium (of thickness L) which can be characterized by a real scalar dielectric constant $\epsilon(\mathbf{x},t)$. We also assume that the optical electric vector can be written as $\text{Re}[\hat{\mathbf{x}}E(\mathbf{x},t)\exp(ikz-i\omega t)]$ where E obeys the modified paraxial wave equation:

$$\left[\frac{\partial^2}{\partial x^2}+\frac{\partial^2}{\partial y^2}+2ik\frac{\partial}{\partial z}+\frac{\omega^2}{c^2}\delta\epsilon(\mathbf{x},t)\right]E(\mathbf{x},t)=0\ , \tag{1}$$

Here $\delta\epsilon(\mathbf{x},t)=\epsilon(\mathbf{x},t)-n^2$ is the zero-mean fluctuating part of the dielectric constant that arises because of the spheres in the water. The thickness L in our experiment is in the range of 10–50 μm so that the light sees a purely static medium (no time dependence) on a single pass. Also we can neglect the transverse diffraction of the beam inside the medium. If, in addition, we can neglect the contribution from scattered light to the electric field of the beam at the exit plane, then we can neglect the transverse derivatives in Eq. (1) to obtain

$$E(x,y,L,t)=E(x,y,0)\exp[i\phi(x,y,L,t)]\ , \tag{2}$$

where

$$\phi(x,y,L,t)=\frac{\omega}{2nc}\int_0^L\delta\epsilon(x,y,z,t)dz\ .$$

The transmitted fraction is then the functional projection of the field on the exit plane on the field that would exist in the absence of attenuation. We can express the (time averaged) transmission therefore by

$$T=\frac{\left\langle\left|\int d^2x E^*(x,y,0)E(x,y,L,t)\right|^2\right\rangle}{\left|\int d^2x\ E^*(x,y,0)E(x,y,0)\right|^2}\ , \tag{3}$$

where $d^2x=dx\,dy$ and all integrals extend to infinity. We will assume that $\delta\epsilon(\mathbf{x},t)$ is a (zero-mean) Gaussian random process. The numerator in Eq. (3) reduces to

$$\int d^2x\int d^2\xi|E(x,y,0)E(\xi,\eta,0)|^2\exp\left[-G\int_0^L\int_0^L[C(|\mathbf{x}_0-\boldsymbol{\xi}_0|)-C(|\mathbf{x}-\boldsymbol{\xi}|)]dz\,d\zeta\right]\ , \tag{4}$$

where $\mathbf{x}_0\equiv(0,0,z)$, $\boldsymbol{\xi}_0\equiv(0,0,\zeta)$ and

$$C(|\mathbf{x}-\boldsymbol{\xi}|)=\frac{\langle \delta\epsilon(x,y,z,t)\delta\epsilon(\xi,\eta,\zeta,t)\rangle}{\langle \delta\epsilon^2\rangle}$$

is the equal time correlation function, and $G\equiv(\omega/2nc)^2\langle\delta\epsilon^2\rangle$. We assume a correlation function of the form $C(|\mathbf{x}-\boldsymbol{\xi}|)=\exp(-|\mathbf{x}-\boldsymbol{\xi}|/L_c)$; then the numerator becomes

$$\int d^2x\int d^2\xi|E(x,y,0)E(\xi,\eta,0)|^2\exp\left[-G\int_0^L\int_0^L[\exp(-|z-\zeta|/L_c)-\exp(-|\mathbf{x}-\boldsymbol{\xi}|/L_c)]dz\,d\zeta\right], \tag{5}$$

where L_c, the correlation length, is of the order of 10 μm, much less than the laser beam width ω_0 of 0.7 mm. The last term in the exponent in Eq. (5) gives a correction to the expression which is obtained without it, that is of the order $(L_c/\omega_0)^2$ smaller. Without this term we get

$$T(L)=\exp[-\alpha_\infty(L-L_c+L_ce^{-L/L_c})], \tag{6}$$

where $\alpha_\infty=2GL_c$ is the attenuation constant at large thickness.

We note two points about these approximate results. First, because we assume that $\delta\epsilon$ is a Gaussian random function in space, the average beam transmission in Eq. (3), with Eq. (2) for the exit beam, implies that

$$\langle\phi^2\rangle=-\ln T\ . \tag{7}$$

Of course this phase fluctuation is only within the exit beam pattern itself, Eq. (2) does not include the scattered light at the exit plane. Second, when the beam is much wider than a correlation length, Eq. (5) gives for the rms fluctuation in Eq. (7)

$$\langle\phi^2\rangle=2GL\int_0^L\left|1-\frac{z}{L}\right|C(z)dz\ . \tag{8}$$

For $L\ll L_c$, $\langle\phi^2\rangle$ approaches GL^2, whereas for $L\gg L_c$, $\langle\phi^2\rangle$ approaches $\alpha_\infty L$. This result follows from the fact that the phase ϕ in Eq. (2) undergoes a random walk as it propagates inside the scattering medium. In particular, the exponential decay of the transmission at large thickness is analogous to the fact that the mean-square displacement of a Brownian particle is proportional to time at long times.

IV. RESULTS

The results of fitting Eq. (6) to our data are shown as the solid lines in Fig. 3. The best parameter values obtained from this fit are summarized in Table I. We see that as the particle density increases, the attenuation constant α_∞ and the correlation length increase. The scattering cross section represented by the ratio α_∞/N does not show any significant change with density for samples A, B, and C, but decreases for the higher densities. The error bounds given in Table I are obtained by simultaneous variations of α_∞, L_c, and L_0 from their best fit values until only half of the data points intercept the theoretical fit. An illustration of two such limit curves are shown by curves labeled F in Fig. 3, and which are shown with the same data as in curve A, but shifted by two units vertically for clarity.

V. DISCUSSION

We have assumed that the dielectric function $\delta\epsilon(\mathbf{x},t)$ is real. This approximation is valid if the absorption of beam energy by the medium does not alter the beam shape (we have verified that it does not) and if the attenuation α_{abs} arising from absorption is much less than α_∞ or L_c^{-1}, whichever is least. The following experimental check shows our nonabsorbing approximation to be valid, even had we used strong 515 nm beams where absorption is presumably greater. We attempt to measure the absorption constant of the latex samples using the thermal blooming effect. We assume our beam has a transverse intensity profile of the form $I(r)=I_0\exp(-2r^2/\omega_0^2)$, which gives rise to an easily calculable transverse thermal gradient in the material due to local heating. The thermal gradient creates a refractive index gradient, thereby creating a thermal lens of focal length F. Assuming that the beam length L in the sample is small compared with both the attenuation length and the focal length of the thermal lens, and that heat is only being conducted in the transverse direction, Gordon *et al.* showed that for the above beam profile, this focal length is given by $F=\pi kn\omega_0^2/(\alpha_{abs}P_0Ln')$.[7] Here: k = thermal conductivity (J cm^{-1} s^{-1} K^{-1}), n = refractive index, α_{abs} = absorption constant (cm^{-1}), P_0 = power of

TABLE I. Measured sample densities N and best parameters for fitting Eq. (6) to data of Fig. 3. The symbols are explained in the text.

Sample	N (10^{11} cm^{-3})	α_∞ (μm^{-1})	L_c (μm)	L_0(μm)	α_∞/N (μm^2)
A	1.1 ± 0.1	0.34 ± 0.02	7 ± 4	1.2 ± 2.0	3.2 ± 0.6
B	1.5 ± 0.1	0.45 ± 0.05	8 ± 4	1.3 ± 1.7	3.0 ± 0.6
C	1.9 ± 0.2	0.63 ± 0.07	9 ± 4	2.5 ± 1.5	3.3 ± 0.6
D	3.1 ± 0.4	0.80 ± 0.08	11 ± 5	1.6 ± 1.3	2.6 ± 0.5
E	4.8 ± 0.3	1.00 ± 0.10	12 ± 6	2.2 ± 1.2	2.1 ± 0.4

incident beam (W), $n'=[dn/d(\text{temperature})]$ at room temperature (K^{-1}), and ω_0, L, and F are in cm. However, to increase sensitivity, we make the suspension that we study longer than the attenuation length. If the other assumptions still hold, the expression of Gordon *et al.* need only be multiplied by $(\ln T)/(T-1)$ for this case, provided that heating due to the scattered light can be neglected. Therefore we have been able to set a lower limit on α_{abs} as follows.

We focused an argon laser ($\lambda=515$ nm) to a minimum beam cross-sectional diameter of 3.6 μm in the suspension (resulting in a maximum intensity of 1.7 MW/cm^2) and were unable to detect any thermal lensing effect on the beam. We used a wavelength different from our previous measurement so as to have much higher power. We employed a sample like B in Table I, for which the transmission T equals 0.125 at a thickness $L\cong 8$ μm. With this geometry there will be a significant fraction of the heat energy being transported along the beam axis. This, we estimate, would not alter our limit on α_{abs} by more than a factor of 3. The transmitted beam, collimated by a lens of focal length 15 cm placed 15 cm from the suspension, then passes through a second identical lens placed 5 cm from the first lens, and impinges on the OMA camera 16.5 cm from the second lens. There the $(1/e^2)$ beam diameter was observed to deviate less than 3% from the low power value (~ 0.7 mm) at all powers up to 0.7 W. Using a Gaussian beam propagation analysis we obtain $|F|\geq 0.44$ mm from this observation. With this limit for F, and the following parameter values: Refractive index $n=n_{\text{water}}+0.1(n_{\text{sphere}}-n_{\text{water}})=1.357$, $P_0=0.7W$, $k\sim 0.597$ Wm^{-1}K^{-1}, and $n'\sim -1.1\times 10^{-4}$ K^{-1} (the value for water alone); we obtain the satisfying result that the attenuation α_{abs} due to absorption is less than 4.5 mm^{-1}.

We checked that the transmission of the latex suspension is independent of intensity so that no nonlinear optical effects (e.g., electrostrictive effect)[8] are important. We also checked the absorption constant of the dye solution after the five sets of measurements, to find that it differed by at most 0.2%. The absorption constant (0.501 mm^{-1}) of the dye used is much smaller than the attenuation constant of the latex suspensions so that the relative error in the scale reading of the dye solution is negligible. The background intensity is much weaker than the transmitted intensity at transmissions above the right-pointing arrows in Fig. 3. Therefore, we rule out multiple scattering as a contributor to this nonexponential behavior. To check whether this behavior is a surface effect due to clustering of particles on the glass windows of the cell, we studied the sample under a microscope. We could just resolve individual spheres at an edge where they were pinned. Their Brownian motion was too fast to render them visible elsewhere; no stationary spheres or clusters could be seen. In fact we could see no light scattering centers at the window. As another check we performed the same measurements with a concentrated dye solution ($\alpha_d\sim 83$ cm^{-1}) in cell $C1$, and found perfect exponential decay. To test the sensitivity of our results to the exact form of the correlation function, we performed a curve fitting with another correlation function of the form $C'(|\mathbf{x}-\boldsymbol{\xi}|)=\exp(-\pi|\mathbf{x}-\boldsymbol{\xi}|^2/4L_c^2)$ which gives

$$T(L)=\exp\{-\alpha_s[\operatorname{erf}(x)L-2L_c(1-e^{-x^2})/\pi]\}\,, \tag{9}$$

where $x=\sqrt{\pi}L/2L_c$. In our curve fitting, we made the approximation $\operatorname{erf}(x)\cong\tanh(5x/4)$, correct to within 1%. A summary of the best parameters and their fitting limits is given in Table II.

Our theoretical treatment neglected the transverse derivatives in Eq. (1) which govern not only the diffraction of the Gaussian beam, but the diffraction of the scattered light as well. We have redone our analysis treating these derivatives in perturbation theory. The result is a fractional correction of the order of $(\lambda\alpha_s L^2/L_c^2)^2$ to Eq. (6) for the transmission T. This corresponds to a maximum correction of about 30% at the extreme low transmission points.

We also estimated the "beam-size" correction which, we noted previously, arises because we neglected the last term in the exponent in Eq. (5). Using the expression above Eq. (9) as the correlation function, we found the lowest-order fractional correction to be of the order $L_c^2/(\omega_0^2|T\ln T|)$ which, for our geometry is much larger than the diffraction corrections. In Fig. 3, the points where this beam size correction is 100% is indicated by left-pointing arrows.

At small thickness in sample B, the scattered light is strongly peaked within a 3° radius cone about the forward direction where, presumably, it consists mainly of singly-scattered photons. This structure factor [which is approximately proportional to the scattered intensity $I(0)$] in the near forward direction is well approximated by a Gaussian function plus a constant and the correla-

TABLE II. Measured sample densities N and best parameters for fitting Eq. (9) to data of Fig. 3. The symbols are explained in the text. Measurements of the structure factor in the near forward direction gives a correlation length of 8 ± 2 μm for sample B and 7 ± 2 μm for a sample with particle density one-fifth of that of sample B.

Sample	N ($\times 10^{11}$ cm^{-3})	α_s (μm^{-1})	L_c (μm)	L_{cc} (μm)	α_s/N (μm^2)
A	1.1 ± 0.1	0.33 ± 0.03	9 ± 5	0.9 ± 2.8	3.0 ± 0.6
B	1.5 ± 0.1	0.44 ± 0.03	10 ± 4	1.4 ± 1.3	2.9 ± 0.6
C	1.9 ± 0.2	0.60 ± 0.07	12 ± 4	2.3 ± 1.2	3.2 ± 0.6
D	3.1 ± 0.4	0.75 ± 0.10	14 ± 5	1.8 ± 0.8	2.4 ± 0.5
E	4.8 ± 0.3	0.92 ± 0.11	14 ± 6	2.4 ± 1.2	1.9 ± 0.3

tion function obtained by Fourier transform suggests [according to the correlation function above Eq. (9)] a correlation length in the scattering medium of 8 ± 2 μm, in agreement with the L_c we find from our model.

There are three types of forces contributing to the interaction between the particles. The first is the hard sphere collision between the particles which gives a correlation length, according to the Percus-Yevick approximation,[9] which is approximately that of the particle diameter. This is different from what we observe in the near forward direction. The second is the hydrodynamic interaction which is dependent on the density of the particles. We have measured the structure factor in the near forward direction for a suspension with particle density one-fifth of that of sample B and obtained the correlation length as 7 ± 2 μm. This suggests that the third kind of interaction, the electrostatic force, is dominant in our suspensions. This also agrees with our dc conductivity measurements since the measured conductivity is two orders of magnitude higher than that of water.

VI. SUMMARY

In summary, we have observed experimentally a strong deviation from Bouguer's law of exponential beam attenuation in the low-intensity limit. These data are very well fitted by a model which assumes Gaussian random fluctuations in the dielectric function that have a correlation length longer than the attenuation length. This correlation length agrees with that estimated from the angular spectrum of the scattered light. We verified that multiple scattering, thermal blooming, surface clustering effects, and nonlinear optical effects do not contribute to this deviation from exponential attenuation.

ACKNOWLEDGMENTS

This research was supported by the U. S. Air Force Office of Scientific Research and by the National Science Foundation under Grant No. ECS-8821507.

---

[1]W. E. Knowles Middleton in *Dictionary of Scientific Biography*, edited by Charles C. Gillispie (Charles Scribner's Sons, New York, 1970.)

[2]A. Ishimaru and Y. Kuga, J. Opt. Soc. Am. **72**, 1317 (1982).

[3]G. Zaccinti and P. Bruscaglioni, J. Mod. Opt. (UK) **35**, 2, 229 (1988).

[4]Model ϕ11 *p*H meter, Beckman Instruments, Inc.

[5]Model 7509, NSG Precision Cells, Inc.

[6]Model 1205A, Princeton Applied Research.

[7]J. P. Gordon, R. C. C. Leite, R. S. Moore, S. P. S. Porto, and J. R. Whinnery, J. Appl. Phys. **36**, 3 (1965).

[8]P. W. Smith, A. Ashkin, and W. J. Tomlinson, Opt. **6**, 284 (1981).

[9]W. Hess and R. Klein, Adv. Phys. **32**, 173 (1983).

Appendix IV

Direct determination of electron mobility in photorefractive $Bi_{12}SiO_{20}$ by a holographic time-of-flight technique

J. P. Partanen, J. M. C. Jonathan,[a] and R. W. Hellwarth
Departments of Physics and Electrical Engineering, University of Southern California, Los Angeles, California 90089-0484

(Received 20 August 1990; accepted for publication 1 October 1990)

The time development of a photorefractive grating created by intersecting 30 ps (532 nm) beams in a well-characterized $Bi_{12}SiO_{20}$ crystal (in a static field around 1 kV/cm) unambiguously reveals the mobility of photoexcited electrons to be 0.24 ± 0.07 cm^2/V s through what is essentially a "time-of-flight" measurement.

Electrical measurements of the mobility of photoexcited carriers in photorefractive insulating crystals have been inconsistent and difficult to interpret, in part because of electrode potentials, surface currents, and hot carriers. Mobility values from 5×10^{-5} to 3 cm^2/V s have been reported for undoped n-type cubic $Bi_{12}SiO_{20}$ (n-BSO) from the photocurrent measurements.[1-3] Here we report holographic time-of-flight measurement of electron drift mobility μ, finding 0.24 ± 0.07 cm^2/V s. The only previous holographic time-of-flight measurement of the mobility of photorefractive carriers known to us is that of Pauliat *et al.*[4] who found values around 10^{-2} cm^2/V s for the carriers of unknown charge sign in three cubic, iron-doped $Bi_{12}GeO_{20}$ crystals. The technique we report here is similar to that employed in Ref. 4 except that our carriers drift under the influence of a static applied voltage V_0 rather than an alternating one, and we excite the carriers with an essentially instantaneous 532 nm pulse ($\simeq$30 ps, 1 μJ/cm^2), rather than with a cw beam.

Described briefly, our technique for observing drift mobility works as follows. A density "grating" $n(x,t)(\cong n_0(t) + \mathrm{Re}[n_1(t)\exp(ikx)])$ cm^{-3} of photoexcited carriers (electrons here) is initially superposed on the grating of ionized deep traps from which the carriers were instantaneously excited. This grating $n(x,t)$ drifts subsequently under the influence of the x-directed static uniform electric field E_0. Before significant diffusion takes place, we observe the rise and fall of the amplitude E_1 of the Coulomb electric field grating ($\mathrm{Re}[E_1(t)\exp(ikx)]$) caused by the movement of the electron grating from coincidence, to anticoincidence, and back to coincidence with the stationary grating of ionized traps. ($E_1 \ll E_0$) The time for this rise of the Coulomb field grating (observed here to be $\approx10^{-5}$ s) is evidently $\pi/(\mu E_0 k)$, where the grating wave vector **k** equals [2π/grating period]. Therefore, we are justified in calling our measurement a direct "time-of-flight" mobility measurement. We monitor $E_1(t)$ by observing the Bragg scattering of a weak laser beam from the refractive index grating $\Delta n(x,t)$ that E_1 causes, via the electro-optic effect: $\Delta n(x,t) = \mathrm{Re}[-(1/2)n^3 r E_1 \exp(ikx)]$. Here n is the linear refractive index and r is the effective electro-optic coefficient for the geometry. We also monitor E_0 via the electro-optic effect. In the following sections, we first outline a simple theory which includes the effects of electron diffusion and recombination, and also the effects of the spatial variation of the mobility. We then review the mobility experiments which we performed as described above on a $5\times5\times5$ mm^3 single crystal of nominally undoped n-type $Bi_{12}SiO_{20}$ of high optical quality, grown by Sumitomo Inc., and well characterized by the various experiments described in Ref. 5 where this crystal was referred to as SU1.

We may obtain a more precise expression for the form of $|E_1(t)|^2$, which the Bragg-scattered 633 nm beam monitors, by using the Poisson equation

$$ikE_1 = e(N_1 - n_1)/\epsilon, \tag{1}$$

where ϵ is the dielectric constant of the crystal, e is the (positive) electronic charge, and $N_1(t)$ cm^{-3} is the (complex) amplitude of the spatially sinusoidal density grating of ionized traps. Since we excite many fewer electrons ($\simeq10^{12}$ cm^{-3}) than the dark density N_A of ionized traps ($\simeq10^{16}$ cm^{-3} from Ref. 5) we may assume that N_1 obeys a simple equation for direct recombination:

$$\partial N_1/\partial t = -n_1/\tau, \tag{2}$$

where τ is the usual electron recombination time, which we have measured by direct observation of photocurrent decay to be 80 ± 5 μs. Initially $N_1(0) = n_1(0)$ (before the electrons have moved) and $E_1(0) = 0$. We assume that the subsequent electron current density $j(x,t)$ is in the x direction and is related to the electron density n by the usual equation representing drift and diffusion:

$$j(x,t) = \mu e n[E_0 + \mathrm{Re}(E_1 e^{ikx})] + \mu k_B T \partial n/\partial x. \tag{3}$$

Here k_B is the Boltzmann constant and T the temperature. Our experiments are in the limit of low photoexcitation where we see only the terms in j which are linear in the energy flux U J/cm^2 of the 532 nm excitation pulse. Since both E_1 and n are linear in U in this limit, we do not observe the second term of (3). The unimportance of this term is confirmed by our theory which predicts $|E_0| \ll |E_1|$ for our experimental conditions: $U\approx10^{-6}$ J/cm^2. Omitting this small term allows us to eliminate j from (3) by using the continuity equation

$$\partial j/\partial x = e(\partial n/\partial t + n/\tau) \tag{4}$$

to obtain for the complex amplitude n_1 of the density grating

[a]Permanent affiliation: Institut d'Optique, U. A. CRNS, Bat. 503, B. P. 43, 91406, Orsay, France.

 0003-6951/90/492404-03$02.00

$$n_1(t) = n_{10} e^{-\Gamma t}, \tag{5}$$

where $n_{10} = n_1(0)$ and

$$\Gamma \equiv \Gamma' + i\Gamma'' = \tau^{-1} - ik\mu(E_0 + ikk_B T/e). \tag{6}$$

With this in (2) we have immediately for the desired Coulomb field grating amplitude

$$E_1(t) = E_\infty (1 - e^{-\Gamma t}), \tag{7}$$

where $E_\infty = -\mu e n_{10}(E_0 + ikk_B T/e)/(\epsilon\Gamma)$.

In our experiment we arranged the grating period k to be 670 cm^{-1}. Then $kk_B T/e$ is 17 V/cm which is much smaller than the fields E_0 (300–2500 V/cm) which we applied to the crystal. Also $(k\mu\tau)^{-1}$ is 77 V/cm in our experiment. Therefore, Γ is nearly $(-ik\mu E_0)$ which creates the sinusoidal rise and fall of $|E_1|^2$ explained in our introduction above. The relative dielectric constant ϵ/ϵ_0 of our BSO sample (called SU1 in Ref. 5) was 56 so that, for the approximately 1.6×10^{12} cm^{-3} electrons initially excited by the 532 nm intensity grating, we expect from (7) that $|E_1|$ will have a maximum value near 80 V/cm and will not depend much on any variation in E_0, μ, or τ that may occur in our experiment.

We have actually observed more damping in the oscillatory behavior of $|E_1|$ versus time than is predicted by (7). We can, however, obtain an excellent agreement with experiment which we document below if we assume that the mobility μ varies randomly with position x in the crystal on a scale larger than a grating spacing but with a correlation length much smaller than any dimension of the Bragg-scattering region. The total Bragg-scattered (phase-matched) 633 nm signal is essentially a coherent superposition of the radiation generated by the electro-optic effect, and hence has a power proportional to $|\int dx^3 E_p(x)E_1(x)|^2$, where E_p is the amplitude of the 633 nm beam scattered, and the integral is taken over the volume of the crystal. We assume that $E_1(x)$ varies through the variation of $\mu(x)$ and Γ in (7), and then average over the deviations $\delta\mu$ of μ from its average $\bar{\mu}$. For simplicity we assume that $\delta\mu$ is a Gaussian random variable and so has the property that $\langle \exp(i\beta\delta\mu)\rangle = \exp(-(1/2)\beta^2\langle\delta\mu\rangle)$. Neglecting the variations in E_∞ arising from $\delta\mu$ (for reasons explained above) we evaluate the foregoing space integral using (7) for E_1 to find directly that the intensity I_S of the Bragg-scattered signal is predicted to obey

$$I_S(t) = I_\infty |1 - \exp[-(\beta\bar{\mu}t)^2 C^2/2 + i\beta\bar{\mu}t - t/\tau]|^2, \tag{8}$$

where $\beta \equiv kE_0 + ik^2 k_B T/e$ and $C^2 \equiv \langle(\delta\mu)^2\rangle/\bar{\mu}^2$ is a parameter describing the fractional fluctuation of mobility throughout the crystal. We find below that taking C to be 0.42 makes (8) to fit all our data to within experimental error. This is not an unreasonable amount of fluctuation in mobility, given the uncontrolled nature of the electron donors and of the impurities in the growth process. The infinite-time asymptote I_∞ is proportional to $|E_\infty|^2$.

Our experimental arrangement is diagrammed in Fig. 1. The beam expander B–E and beamsplitter BS1 form two

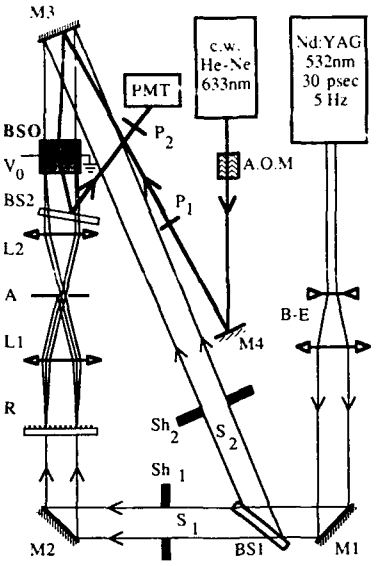

FIG. 1. Experimental arrangement for the holographic time-of-flight measurement.

beams of 30 ps 532 nm pulses labeled S_1 and S_2 which are shuttered by Sh_1 and Sh_2. The beam S_1 excites the initial grating of photoelectrons, its flux having been spatially modulated to equal $U[1 + \cos(kx)]$ in the BSO sample, by transmission through the Ronchi ruling R and the spatial filter (compromising lenses $L1$ and $L2$ separated by aperture A). The 0 and 1 orders were used in our experiment to make $k = 670$ cm^{-1} (a grating period of 93 μm). The experimentally employed range of U was between 0.1 and 5 $\mu J/cm^2$. The second 532 nm beam S_2 was used to erase previously written photorefractive gratings before the excitation. Both beams had an intensity that was uniform over the He-Ne probe beam to within 5%.

The variation in time of the photorefractive gratings in the BSO sample was monitored by the (1.2 mm diameter) 633 nm He-Ne laser beam controlled by an acousto-optic modulator (AOM), and linearly polarized by P_1 at such an angle as to make its Bragg-diffracted signal orthogonally polarized to the nearby directly transmitted beam. The polarizer P_2 was then effective in eliminating ordinary scattered light from the Bragg-diffracted signal recorded by the photomultiplier (PMT).

The voltage V_0, which was applied to the BSO sample to create the drift in the x direction of the photoexcited electrons, was carefully coordinated in time with the shutters Sh_1 and Sh_2 and the acousto-optic modulator to minimize the residual space charge. The polarization of the primary 633 nm beam that was transmitted through the sample was measured in order to determine the applied electric field E_0 via the electro-optic effect as described in Ref. 6. We found that E_0 was spatially uniform and typically 70% of V_0/d, where d was the distance between (5 mm) the coated electrodes. We believe that the accuracy of the electric field measurement was ±25%. The direction (x) of E_0 was parallel to the (1,1,0) crystal axis. The 532 nm beams were parallel to the $(1,\bar{1},0)$ axis.

The diffracted 633 nm intensity versus time averaged

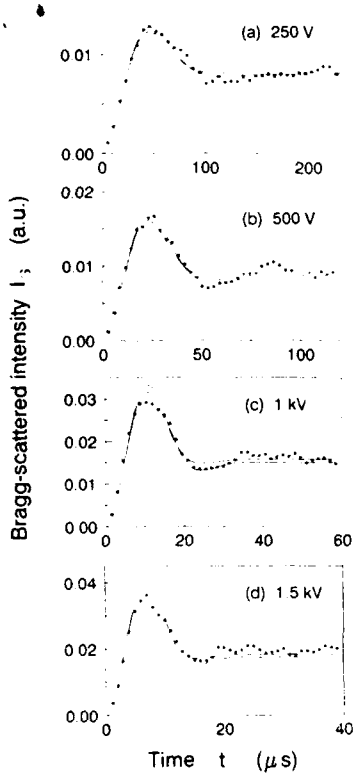

FIG. 2. Bragg-scattered intensity of the 633 nm beam vs time t from the BSO sample after the picosecond photoexcitation pulse when four different voltages were applied across the sample. Also two best-fit curves are shown.

over about 50 shots is shown in Fig. 2 for four different applied voltages to the sample "SU1" of n-type BSO.[6] The two solid curves drawn over each data set correspond to two choices for the set of parameters $(C, |\beta\overline{\mu}|, I_\infty)$ in a plot of (8). The independently observed recombination time $\tau = 80\ \mu$s and a small parameter δ in $\beta\overline{\mu} = |\beta\overline{\mu}|e^{i\delta}$ (deduced from the electric field measurements) were used in all of the solid curve plots. The solid curve with the lowest maximum corresponds to $C = 0.42$ in each case along with the least-squares values of $|\beta\overline{\mu}|$ and I_∞ listed in Table I. The other solid curve is for $C = 0.35$ in each case, value which increases the rms deviation of the data by 20%. The errors listed in Table I for $(\beta\overline{\mu})$ and I_∞ reflect the new best values when $C = 0.35$ is used. The variation in I_∞ is mainly caused by the differences in the excitation energy fluxes (I_∞ proportional to $|U|^2$).

TABLE I. Spatial average $\overline{\mu}$ of photoelectron mobility as obtained by adjusting $|\beta\overline{\mu}|$ and I_∞ to obtain the best fit of (8) to the data of Fig. 2, for four values of applied voltage V_0 to $Bi_{12}SiO_{20}$ sample SU1. The least-squares error value $C = 0.42$ was used in (8) for the computation.

V_0 (kV)	U (μJ/cm^2)	E_0[a] (kV/cm)	$\lvert\beta\overline{\mu}\rvert$ (10^3 s^{-1})	I_∞ (10^{-4})	$\overline{\mu}$ (cm^2/Vs)
0.25	0.78	0.31	50.8 ± 0.5	80 ± 2	0.245
0.50	0.73	0.67	105 ± 2	90 ± 3	0.234
1.00	0.93	1.38	230 ± 5	157 ± 7	0.249
1.50	0.99	2.17	362 ± 12	183 ± 9	0.249

[a]These values, measured as explained in text, have relative uncertainty 5% and absolute uncertainty of 25%.

One sees that none of the four fields gives a value for the mobility $\overline{\mu}$ that deviates by more than 5% from their mean value 0.24 cm^2/V s. We feel that the uncertainty in the true value for this sample arises mainly from our estimated 25% uncertainty in the absolute value of E_0 which we calculated from the polarization shift of the 633 nm beam (caused by the electro-optic effect) assuming the electro-optic coefficient r_{41} of our sample to be the generally accepted value 4.4 pm/V for BSO at 633 nm.[7] Therefore we have assigned an estimated uncertainty of ± 0.07 cm^2/V s to our mobility determination.

In any case, we note that, had we simply measured the time for the signal I_S to reach its peak, and equated that time to $\pi/(\overline{\mu}E_0 k)$ we would have obtained the same value for $\overline{\mu}$ to within 5% in each case. Our more careful analysis of the data should not cloud the fact that we have essentially a "time-of-flight" measurement of the mobility here. The most interesting insight to come from our data analysis is that our data fit the theoretical expression (8) much better if we assume that the macroscopic mobility-field product (μE_0) fluctuates by $\pm 40\%$ from place to place in the crystal. By "macroscopic" we mean to imply that fluctuations on a scale smaller than the grating period do not affect our results. Since we could not see variations in E_0 larger than $\pm 5\%$ using the electro-optic effect, we feel justified in assuming that the mobility μ itself was varying from place to place in the crystal by roughly $\pm 40\%$.

We note also that the value for the product $(\mu\tau)$ for the electrons in SU1 was inferred from the k dependence of grating erasure rates in Ref. 6. With the value $\tau = 80 \pm 5$ μs which we have measured by photocurrent decay,[8] we would predict $\mu = 0.17 \pm 0.1$ cm^2/V s, a value consistent with our more accurate finding here. If we assume the quantum efficiency for photoelectrons to be $\simeq 85\%$ as estimated in Ref. 6, then our new mobility value correctly predicts the absolute value of current in the photocurrent experiment with a 30 ps 532 nm light pulse.[8] The variation of I_∞ in Table I is also consistent with that expected using the parameters of Ref. 6 in (8).

This research was supported by the U. S. Air Force Office of Scientific Research under contract No. F 49620-88-C-0027 and by the National Science Foundation under grant No. ECS-8821507.

[1] S. L. Hou, R. B. Lauer, and R. E. Aldrich, J. Appl. Phys. **44**, 2652 (1973).
[2] B. Kh. Kostyuk, A. Yu. Kudzin, and G. Kh. Sokolyanskii, Sov. Phys. Solid State **22**, 1429 (1980).
[3] G. Le Saux and A. Brun, IEEE J. Quantum Electron. **QE-23**, 1680 (1987).
[4] G. Pauliat, A. Villing, J. C. Launay, and G. Roosen, J. Opt. Soc. Am. B **7**, 1481 (1990).
[5] F. P. Strohkendl, P. Tayebati, and R. W. Hellwarth, J. Appl. Phys. **66**, 6024 (1989).
[6] J. M. C. Jonathan, R. W. Hellwarth, and G. Roosen, IEEE J. Quantum Electron. **QE-22**, 1936 (1986).
[7] A. R. Tanquay, Jr., Ph.D. thesis, Yale University, New Haven, CT, 1977.
[8] J. P. Partanen, P. Nouchi, J. M. C. Jonathan, and R. W. Hellwarth (unpublished).

Appendix V

ANNALES DE PHYSIQUE
Colloque n°1, supplément au n°1, Vol. 16, février 1991 135

CHARGE TRANSPORT AND HOLOGRAPHIC DETERMINATION OF THE MOBILITY OF THE CHARGE CARRIERS IN PHOTOREFRACTIVE BSO

J. PARTANEN, P. NOUCHI, J.M.C. JONATHAN* and R.W. HELLWARTH

Departments of Physics and Electrical Engineering, University of Southern California, Los Angeles CA 90089-0484, U.S.A.
**University of Southern California and Institut d'Optique, URA CNRS n°14, Bat. 503, BP. 147, F-91403 Orsay Cedex, France*

RESUME Nous présentons une mesure holographique du temps de vol des porteurs de charge dans les matériaux photoréfractifs qui permet d'accéder directement à leur mobilité. Nous l'avons expérimentée sur un échantillon de $Bi_{12}SiO_{20}$ préalablement caractérisé par différentes techniques. Nos résultats montrent que la vitesse d'entrainement des porteurs est proportionnelle au champ electrique qui leur est appliqué (de 200 à 2000 Vcm^{-1} environ). On trouve alors, indépendamment de tout autre paramètre du matériau, une mobilité de 0.24 ± 0.07 $cm^2V^{-1}s^{-1}$. Nous présentons aussi des mesures de photocourants transitoires confirmant ce resultat.

ABSTRACT We present a holographic time-of-flight technique to access directly the mobility of the photoexcited charge carriers in photorefractive materials. We experimented it on a previously well characterized sample of $Bi_{12}SiO_{20}$. Our data show a linear dependence of the drift velocity versus applied electric field in our experimental range (≈200 to 2000 Vcm^{-1}). We find, independantly of any other material parameter, a mobility of 0.24 ± 0.07 $cm^2V^{-1}s^{-1}$ which is consistent with other transient photocurrent experiments also presented here.

I-INTRODUCTION

The photorefractive effect, known to allow near real time image processing and phase conjugation at very low illumination has been intensively investigated in semi-insulating materials like $BaTiO_3$, $LiNbO_3$, $Bi_{12}SiO_{20}$ (BSO). There is now a general agreement on the mechanism of the effect: The light induced generation of free carriers from photorefractive sites, followed by their transport and recombination leads to a charge redistribution and a space charge Coulomb field which is turned into an index variation through the linear electrooptic effect. However, neither the nature of the photorefractive sites nor the charge transport mechanism are yet fully understood. The study, mostly in BSO, of the transient photocurrents generated by laser pulses under an applied dc electric field provides estimates for the mobility of the charge carriers ranging from $5\ 10^{-5}$ to 3 $cm^2/(Vs)$[1-2]. Values have also been obtained for the diffusion length (which caracterizes the product of the mobility μ by the lifetime τ of the charge carrier), from beam coupling or decay of the diffraction efficiency of a photorefractrive grating under cw-illumination[3]. Using those values, an estimate of the mobility in BSO, as high as 50 $cm^2/(Vs)$, was obtained from the build-up of a grating of short period after a 28ps pulse[4]. Recently, Pauliat et al. obtained a value $4\ 10^{-3}$ $cm^2/(Vs)$ for a $Bi_{12}GeO_{20}$ (BGO) crystal from the time dependence of the beam coupling gain in a two wave mixing experiment with a rectangular A.C. field applied to the crystal[5]. To our knowledge, this was the first published time-of-flight technique. These different methods give very low values for the mobility. Using them, the mean free path of a charge carrier, estimated in a simple model where its movement is limited by collisions would be a fraction of an angstrom (much smaller than any interatomic distance in the crystal). The technique we describe here is similar to that published by Pauliat except that our carriers drift under the influence of a static electric field after having been photoexcited by an essentially instantaneous 532 nm pulse (≈ 30 ps, $1\mu J/cm^2$) rather than by a cw illumination.The success of this versatile technique requires the possibility for the

photoexcited carrier to drift at least one holographic grating period before recombining. The pulse energy should be able to induce a Coulomb field grating strong enough to be observed through the electrooptic effect but weak enough to avoid any saturation of the excitation and transport processes. From a standard photocurrent experiment, we find the experimental conditions in which these requirements are fulfilled. We report our result in the case of a previously well characterized crystal and show that our values for the mobility are consistent with the values projected from our photoconductivity data.

In section II, we establish the principle of the holographic time-of-flight method, within the simplest band conduction model, in a regime of low illumination. In Section III, we outline the results of a transient photocurrent experiment that set the proper experimental conditions for the time-of-flight experiment. The apparatus and results of the time-of-flight experiment are described in section IV. In section V, we compare these results to those implied from our photocurrent measurements and summarize our conclusions.

II-THE HOLOGRAPHIC TIME-OF-FLIGHT METHOD.

Consider a phorotrefractive crystal, illuminated by the intensity pattern

$$I(t,z) = I_0(t)\left(1+\mathscr{B}e\{m\exp(ik.z)\}\right) \qquad (1)$$

resulting from the interference of two short laser pulses of duration τ_p. In the simplest model for the photorefractive effect, including a single type of photorefractive sites of density N_D, and a single type of charge carriers (e.g., electrons), we study the dynamics of the ionized site density N_D^i, the density n of conduction band electrons and the electric field E inside the crystal.

The pulse duration τ_p is assumed to be shorter than any other caracteristic time, so that neither recombination nor noticeable charge movement occurs during τ_p: no space charge field builds-up during the pulse. If the energy of the pulse is small enough ($SI\tau_p<<1$), the initial conditions may be written as :

$$\left.\begin{aligned} N_D^i(z,\tau_p) &= N_A + SI_0\tau_p(N_D - N_A)\left(1+\mathscr{B}e\{m\exp ikz\}\right) \\ n(z,\tau_p) &= SI_0\tau_p(N_D - N_A)\left(1+\mathscr{B}e\{m\exp ikz\}\right) \end{aligned}\right\} \qquad (3)$$

After the pulse (i.e., in the dark) the evolution of the system, is controled by four equations. The rate equation describes the recombination process :

$$\frac{\partial N_D^i(z,t)}{\partial t} = -\gamma N_D^i(z,t)\,n(z,t) \qquad (3)$$

where γ is the recombination rate constant. Assuming free electron transport in the conduction band, the current equation includes both diffusion and drift components near thermal equilibrium at temperature T,

$$\vec{j}(z,t) = n(z,t)\,e\,\mu\,\vec{E}(z,t) + \mu\,k_BT\;\vec{\nabla}n(z,t) \qquad (4)$$

where e is the charge (positive) of the electron, μ its mobility (positive) and k_B the Boltzmann's constant. The continuity equation for the photo-excited electrons is,

$$\frac{\partial\, n(z,t)}{\partial t} + \gamma N_D^i(z,t)\,n(z,t) = \frac{1}{e}\vec{\nabla}.\vec{j}(z,t). \qquad (5)$$

The Poisson equation describes the electric field resulting from both electron and ionized donor densities

$$\vec{\nabla}\vec{E}(z,t) = \frac{e}{\varepsilon_{DC}}\left(N_D^i(z,t) - N_A - n(z,t)\right) \qquad (6)$$

where ε is the permeability of the crystal and N_A the density of acceptors required by electrical neutrality. Assuming a small modulation m, Eqs. (3) - (6) may be linearized by writing the spatially variable quantities as the sum of a constant term and of a small sinusoidal one :

$$\left.\begin{aligned} N_D^i(z,t) &= N_0(t) + \mathcal{B}_e\{N_1(t)\exp(ikz)\} \\ n(z,t) &= n_0(t) + \mathcal{B}_e\{n_1(t)\exp(ikz)\} \\ E(z,t) &= E_0 + \mathcal{B}_e\{E_1(t)\exp(ikz)\} \end{aligned}\right\} \qquad (7)$$

where E_0 is a dc electric field applied to the crystal. A system of linear differential equations is obtained. Here, we solve it, in the case of low energy pulses i.e when the conditions $n_0(\tau_p) << N_A$ and $n_0(t) << n_s \equiv \frac{\gamma N_A \varepsilon}{\mu e} + k^2 \frac{\varepsilon k_B T}{e^2}$, are satisfied. Both n_0 and E_1 are then small and the terms in n_0 may then be neglected in the equations for the spatially varying components of (7). Two simple differential equations are obtained :

$$\left.\begin{aligned} \frac{\partial n_1(t)}{\partial t} + \left(\gamma N_A\left(1+\frac{k^2}{\kappa^2}\right) - ik\mu E_0\right) n_1(t) = 0 \\ \frac{\partial E_1(t)}{\partial t} = \gamma N_A \frac{e}{\varepsilon \kappa^2}(k_E + ik) n_1(t) \end{aligned}\right\} \qquad (8)$$

with :
$$\kappa^{-2} = \mu\tau_r \frac{k_B T}{e}, \quad k_E = E_0 \frac{e}{K_B T} \qquad (9)$$

They are easily solved as

$$\left.\begin{aligned} E_1(t) &= E_\infty\left(1 - e^{-\Gamma t}\right) \\ \Gamma &\equiv \Gamma' + i\Gamma'' \equiv \gamma N_A + k^2\mu\frac{k_B T}{e} - ik\mu E_0 \\ E_\infty &\equiv -\mu\frac{e}{\varepsilon} n_1(0)\frac{E_0 + ik\,k_B T/e}{\Gamma} \end{aligned}\right\} \qquad (10)$$

The electric field shows damped oscillations caused by the superposition of the stationary ion grating upon a grating of free electrons drifting with constant velocity under the influence of the electric field E_0. The oscillations are associated to the successive coincidences and anti-coincidences of these two sinusoidal distributions . They are decaying progressively by diffusion and recombination. If the dc electric field applied to the crystal is strong enough ($k_E > k + \kappa^2/k$), the imaginary part Γ'' of the damping constant may be smaller than the real part Γ'. The free carrier grating may "fly" one or several holographic grating periods before vanishing. Γ'' does not depend on any other material parameters than the mobility itself. It can be accessed by diffracting a laser beam from the crystal. The diffraction efficiency η is proportional to the square of the amplitude of the Coulomb grating E_1:

$$\eta = \eta_\infty \left|1 - e^{-(\Gamma + i\Gamma'')\gamma}\right|^2 \qquad (11)$$

where η_∞ is the value of the diffraction efficiency after damping of the oscillations. This method is a direct illustration of the concept of mobility that states that free carriers move with a speed proportional to the electric field. Measuring Γ'' allows undisputed determination of that mobility. Only, the value of the electric field inside the crystal needs to be correctly evaluated. Before presenting our experimental set-up and fitting our results to equation (11), we summarize our transient photocurrent experiments that set the proper conditions to obtain $\Gamma'' >> \Gamma'$.

III TRANSIENT PHOTOCURRENT EXPERIMENTS.

We studied the time evolution of the photocurrent induced by a picosecond laser pulse in a 5 x 5 x 5 mm^3 crystal by Sumitomo named SU1 in Ref.3 and previously characterized in that paper by fitting two-beam coupling and grating erasure data to the electron-hole competition model. These experiments determine the mobility x lifetime product $\mu\tau$ of the carriers but cannot

access them separately. Our photocurrent experiment will provide an estimate for τ and thereby allow us to estimate the proper grating period for the time-of-flight measurement.

The photocurrent *i(t)* induced by a picosecond pulse was studied with an electric field ($\approx 1 kVcm^{-1}$) applied to the crystal. The arrangement is shown in Fig.1. The light source is a mode locked Nd:YAG laser from which pulses are extracted with a repetition rate of 5 Hz using a Pockels cell. After amplification and frequency doubling, 30 ps pulses at 532nm are obtained. An electromechanical shutter is used to select a single pulse and the laser beam is expanded for uniform illumination of the whole crystal. Two photodiodes PD_1 and PD_2 monitor the incident and transmitted energies. Voltages V_0 up to 1kV can be applied to the crystal by means of silver paint electrodes. The photocurrent is then measured using a carefully designed ciscuit, with short connections to minimize stray inductance, a large high voltage capacitor C and 50Ω coaxial cable. It has a rise time of 1 ns and less than 10% ringing. When a high resolution is needed, the 50Ω cable itself plays the role of the load resistor and is directly connected to the 50Ω input of a 400MHz oscilloscope. For longer time scales and high sensitivities, we use a 100kΩ load resistor connected to the 1MΩinput of the same oscilloscope.

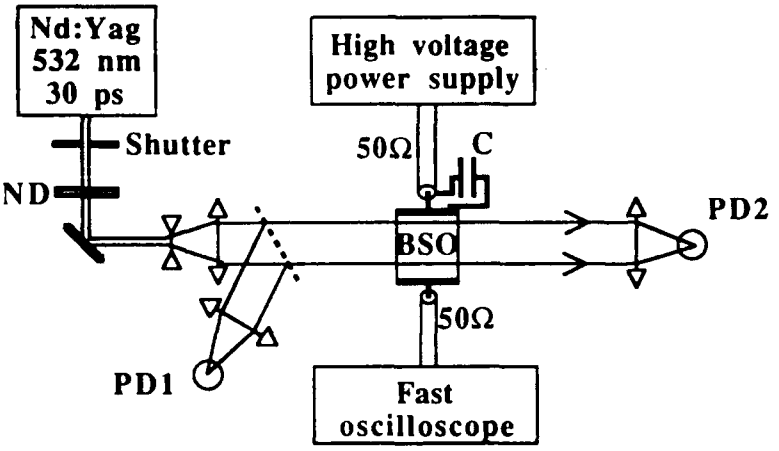

Fig.1 *Experimental set-up for the measurement of transient photocurrents in photorefractive crystals.*

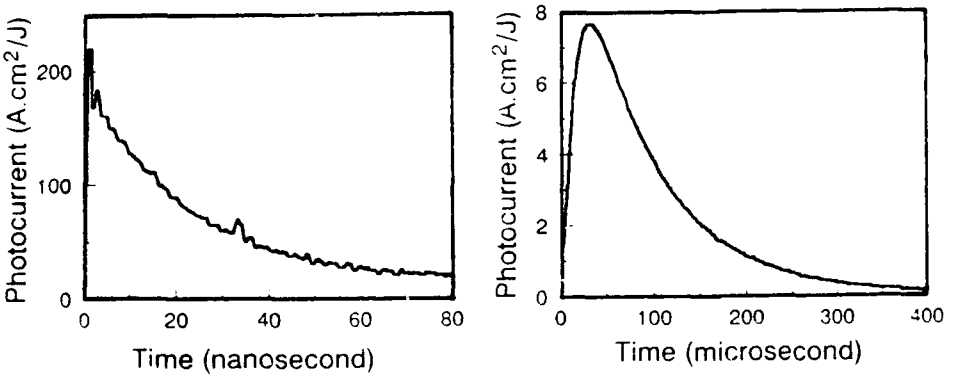

Fig.2 *Transient photocurrent in crystal SU1 after a single 30 ps laser pulse a) fast exponential decay t_1=26±3 ns - b) Slower exponential decay t_2=80±5μs oberved with lower resolution set-up (see text).*

At low fluences ($\leq 30\mu J/cm^2$) the photocurrent shows essentially two exponential decays having time constants of t_1=26±3 ns and t_2=80±5μs (Fig.2).

Although the photocurrent is much smaller during the larger time scale, about 100 times more charges flow inside the crystal during that period of time than during the initial current pulse. The photocurrent data can be conveniently expressed in the form of the average magnitude of the distance $x_a(t)$ travelled by a charge carrier :

$$x_a(t) \equiv \frac{1}{N}\sum_{n=1}^{N}|x_n(t)| \equiv -\frac{d}{Ne}\int_0^t i(t')dt' \qquad (12)$$

Where N is the number density of free charge carriers at the end of the laser pulse. d is the distance between the electrodes and $x_n(t)$ the distance travelled by a charge in the direction of the applied electric field from its original position, up to time t.

We computed $x_a(t)$ by integrating the photocurrent. N was estimated assuming a unit quantum efficiency as in Ref.3, taking into account 20% reflections at the surfaces of the crystal and using an absorption coefficient of 0.74±0.25 cm^{-1} measured by ourselves. The results plotted in Fig.3 using logarithmic scales show two caracteristic shoulders corresponding to the different decay rates.

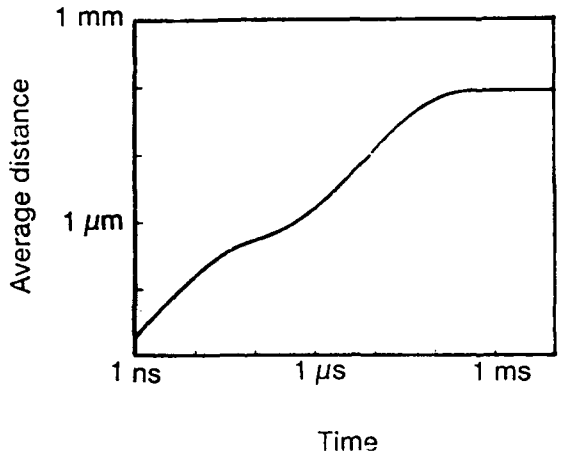

Fig.3 *Average distance $x_a(t)$ travelled by photoexcited charge carriers as a function of time t, calculated fron Eq.12 from our photocurrent measurement at low fulences ($\leq 30\ \mu Jcm^{-2}$) and average applied electric field of 1 $kVcm^{-1}$.*

The decay rates extracted from Fig.2 are consistent with the predictions that can be made unsing the parameters of Ref.3 for SU1 and the electron-hole model. We take t_1 and t_2 as the respective hole and electron recombination times, associating the longest of them with the electrons which are the majority carriers and therefore the majority contributors to $x_a(\infty)$ in that crystal. Relying on the quantum efficiency estimate of 0.86 from Ref.3 for electron excitation, their mobility may be estimated to 0.13±0.07 $cm^2V^{-1}s^{-1}$. The electron and hole $\mu\tau$ products estimated from Fig.2 are also in good agreement with those determined holographically in Ref.3. These photocurrent measurements set the proper experimental conditions for the holographic determination: The grating period has to be large enough to minimize diffusion and still within the average travelled distance of 100 μm with an applied field of 1 kV . The whole transport takes about 100 μsec which sets the approximate time scale for the experiment.

IV THE TIME-OF-FLIGHT EXPERIMENT AND ITS RESULTS.

We experimented the holographic method using the set-up illustrated by figure 4. The light source is the same as in the photocurrent experiment.The beam splitter BS1 provides two

beams S_1 and S_2. S_1 illuminates a Ronchi ruling R imaged on the crystal by a pair of Fourier transforming lenses L_1 and L_2. In the intermediate Fourier plane F, an aperture selects two lowest order spatial frequency waves (0 and +1 or -1) diffracted by R.The crystal is thus illuminated by a sinusoidal distribution of intensity whose period is 93 μm and modulation depth m ≈ 1. The writing beam fluence was 1 $\mu J/cm^2$ which satisfies the low illumination condition ($N_A \approx 10^{16} cm^{-3}$, $n_s \approx 2\ 10^{12} cm^{-3}$) . S_2 is used to erase previously recorded gratings by uniformly illuminating the crystal from the back . Two electronically controlled shutters Sh_1 and Sh_2 insure the single pulse writing of a grating and its erasure. A voltage V_0 is applied to the crystal by means of a power supply which is electronically switched on just before the writing pulse.The crystal is oriented for maximum diffraction efficiency with the grating *k* vector along the (110 direction) and the diffraction efficiency is monitored using a 10 μW He-Ne laser beam. It is linearly polarized by-P_1 so that the polarization of the light, scattered by defects in the crystal is mostly orthogonal to the diffracted beam and can be blocked by the polarizer P_2. This is made necessary by the small grating period used in this experiment. To minimize the generation of charge carriers by the He-Ne beam, an acousto-optic modulator AOM is used to turn the beam on 200μs before the writing pulse from the YAG laser, and turn it off during the erasing phase.

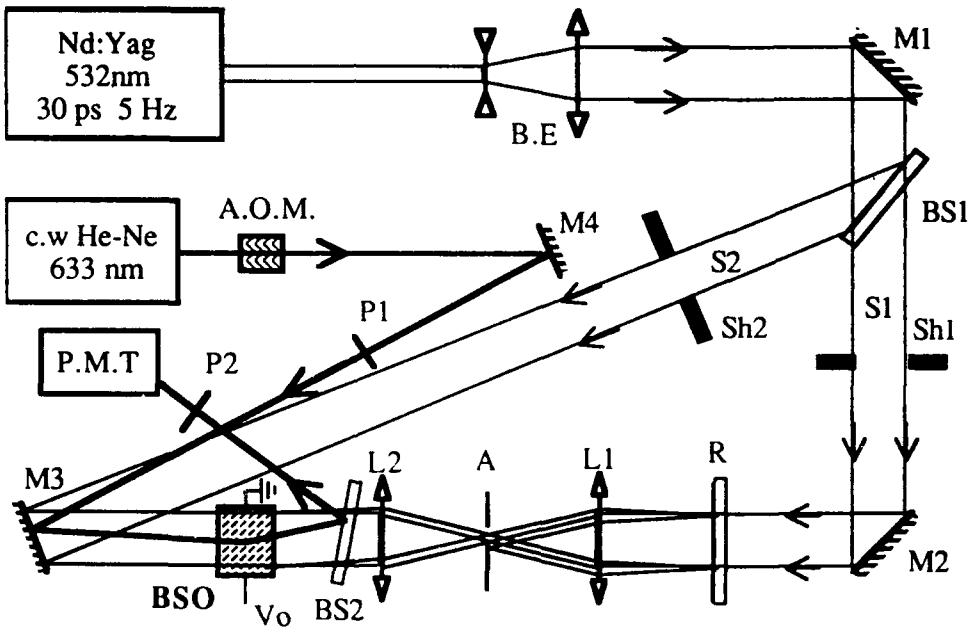

Fig.4 *Experimental arrangement for the time-of-flight holographic mobility measurement.*

A carefull timing allows full decay of the space charge field between successive writing pulse. A P.M.T. measures the time evolution of the weak diffracted signal. To minimize a space charge field build-up, the voltage is connected about a second before the writing pulse, while the crystal is kept in the dark. The noisy signal is averaged over about 50 shots and filtered both electronically at the input of the storage digital oscilloscope and later numerically. The total integration time of this smoothing process is kept smaller than 0.1 times the time at which the diffraction peaks i.e. the time when $x_a(t)$ is half the period of the grating.

Fig.5 shows the experimental time evolution of the diffraction efficiency for "SU1" with V_0 = 1 kV, along with the best fit of these data to equation (11) with parameters μ_{∞},Γ'andΓ''. The real value E_0 of the electric field inside the crystal is needed for the determination of the mobility. It has been frequently observed that E_0 does not equal the ratio of the applied voltage V_0 to the distance *d* between the electrodes. We measured it separately, using the change in the polarisation of the transmitted He-Ne beam caused by the electrooptic effect as described in Ref.6. The values measured for E_0 were typically 0.7 V_0/d, with the coefficient increasing

slightly with V_0. To caracterize the uniformity of this field across the crystal, these measurements were performed using a beam diameter of 0.4 mm (1/3 of the beam size used for the diffraction experiment). E_0 was found to be uniform within 5 % both along and normal to the electric field direction. We also could observe that the electric field E_0 did not change more than 5% during the build-up of the photorefractive grating.

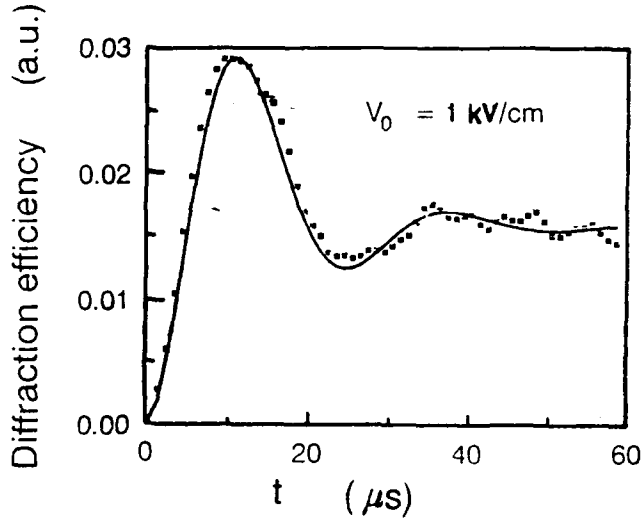

Fig.5 *Time behavior of the diffraction efficiency in SU1 sample after a picosecond excitation pulse. The solid curve is a plot of Eq. 11 with* $\Gamma=8.6\ 10^4\ s^{-1}$ *and* $\Gamma''= 2.42\ 10^5 s^{-1}$ *which gives the best fit to the data.*

The mean electron drift velocity $\bar{v} = \Gamma''/k$,obtained from the fitted values of Γ'' is plotted on Fig.6 as a function of E_0. The linear variation confirms the notion of mobility. From this set of data, we obtain its value μ=0.24 $cm^2V^{-1}sec^{-1}$. The main uncertainty remains here that on the electric field which could be as big as 30%.

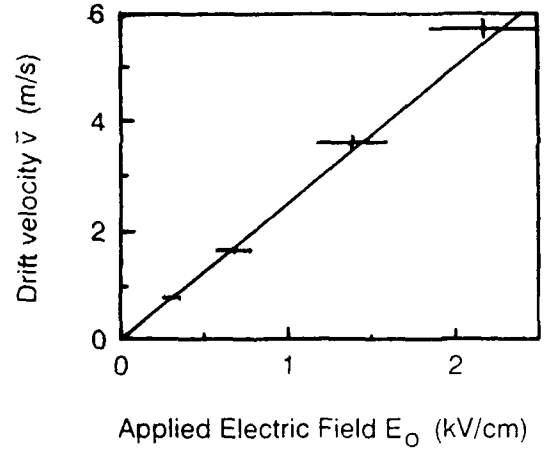

Fig.6 *Mean electron drift velocity versus applied electric field as determined by fitting Eq.11 to four curves as shown in Fig.5.*

We also noticed that contrary to Eq. (10), the damping constant Γ also varies linearly with the electric field E_0. This can be explained by a dispersion in the values of the product μE_0

across the crystal. Our experiments rule out strong nonuniformities of the electric field. However, nonuniformities in the mobility itself would easily result from slight variations in the environmental conditions during the growth of the crystal. This is will be shown in a future publication.

V CONCLUSIONS

In this paper we demonstrate the use of an holographic method to measure photoexcited charge carriers mobilities in photorefractive materials. On a well characterized n-BSO crystal, the conductivity is seen to be ohmic over our experimental range of electric field (200 to 2000 V/cm) and has a value of 0.24 ± 0.07 $cm^2V^{-1}s^{-1}$. We have made two other independent evaluations of the electron mobility in the same sample: an electrical determination from the absolute photocurrent, the absorption coefficient reported here and the quantum efficiency from Ref.3 gives the value 0.13 ± 0.08 $cm^2V^{-1}s^{-1}$. An evaluation based on the measured diffusion length $L_D=\kappa_e^{-1} = 5.8 \pm 2.3$ μm of Ref.3 and our recombination time $t_2=80\pm 5$μs gives a value 0.17 ± 0.1 $cm^2V^{-1}s^{-1}$. All three measurements give essentially the same result which is too small to be explained by collision limited free electron transport in the conduction band. A model of photoexcited carriers hopping between thermally excitable shallow traps as proposed in Ref.7 would eventually explain those values. A study of the temperature dependence of the mobility is now under progress, using the time-of-flight technique.

ACKNOWLEDGMENTS

This research was supported by the U.S. Air Force Office of Scientific Research under contract # F 49620-88-C-0027 and by the National Science Foundation under Grant # ESC-8821507.

REFERENCES

[1] S.L. Hou, R.B. Lauer and R.E. Aldrich, "Transport processes of photoinduced carriers in $Bi_{12}SiO_{20}$",J. Appl. Phys., **44**, 2652 (1973).

[2] B.Kh. Kostyuk, A.Yu Kudzin and G.Kh. Sokolyanskii, "Phototransport in $Bi_{12}SiO_{20}$ and $Bi_{12}GeO_{20}$ single crystals", Sov.Phys. Solid State, **22**, 1429 (1980).

[3] F.P. Strohkendl, P. Tayebati and R.W. Hellwarth, "Comparative study of photorefractive $Bi_{12}SiO_{20}$ crystals", J. Appl. Phys.,**66**, 6024 (1989).

[4] J.M.C.Jonathan, Ph.Roussignol and G.Roosen, "Time resolved build-up of a photorefractive grating induced in $Bi_{12}SiO_{20}$ by picosecond pulses", Opt.Lett.,**13**,224, (1988)

[5] G. Pauliat, A. Villing, J.C. Launay and G. Roosen, " Optical measurement of charge carrier mobilities in photorefractive sillenite crystals", J.O.S.A. B, **7**, 8,1481, (1990).

[6] J.M.C. Jonathan, R.W. Hellwarth and G. Roosen," Effect of applied electric field on the buildup and decay of photorefractive gratings", IEEE J. Qantum Electron., **QE-22**, 1936 (1986).

[7] G. Le Saux and A. Brun, " Photorefractive material response to short pulse illumination", IEEE J. Quantum Electron.,**QE-23**, 1680, (1987).

Appendix VI

PHYSICAL REVIEW B VOLUME 44, NUMBER 4 15 JULY 1991-II

Comparison between holographic and transient-photocurrent measurements of electron mobility in photorefractive $Bi_{12}SiO_{20}$

J. P. Partanen, P. Nouchi, J.M.C. Jonathan,* and R.W. Hellwarth
Department of Electrical Engineering and Department of Physics, University of Southern California, Los Angeles, California 90089-0484

(Received 1 October 1990; revised manuscript received 7 February 1991)

We have developed a time-of-flight technique for measuring the mobility of photoexcited charge carriers in certain crystals exhibiting the electro-optic effect. We used this holographic technique to find that the mobility of photoexcited electrons in a previously well-characterized sample of *n*-type $Bi_{12}SiO_{20}$ is 0.24 ± 0.07 $cm^2V^{-1}s^{-1}$, independent of electric field in our range of observation ($\approx$200–2000 V/cm). We also present results of transient photocurrent measurements. When used with our absorption measurement and previously reported values of the quantum efficiency and mobility-lifetime product, they give two independent estimates of electron mobility that are consistent with our directly measured value.

I. INTRODUCTION

The mobility of photoexcited carriers in photorefractive insulating crystals is a key parameter in determining the response time of a material. However, its reliable measurement has proven to be more difficult than expected. In nominally undoped $Bi_{12}SiO_{20}$ previous measurements using purely electrical experimental techniques have provided conflicting values ranging from 5×10^{-5} $cm^2V^{-1}s^{-1}$ to 3 $cm^2V^{-1}s^{-1}$.[1–4] Similarly conflicting values have been reported for structurally similar $Bi_{12}GeO_{12}$.[2,4] The measurements of Refs. 1 and 2 are based on the transit time of photoexcited carriers through a thin sample, but they do not show the usual top-hat profile[5] of photocurrent, which is easy to analyze. Instead, shapes of current pulses lead to concepts like "dispersive" phototransport[6] for which, strictly speaking, the mobility cannot be defined. The mobility values quoted in Refs. 3 and 4 are based on the absolute magnitude of the photocurrent combined with measurements of the optical absorption coefficient and estimates of quantum efficiency (fraction of absorbed photons creating photocarriers), thus giving only qualitative estimates of the mobility. Purely electrical mobility measurements also suffer from complications caused by electrode potentials, surface currents, and nonuniform electric fields, which can even change during the course of the measurement.

Optical measurements of the range (or diffusion length) of photoexcited charge carriers[7] have also been used to estimate the charge-carrier mobilities of $Bi_{12}SiO_{20}$ and $Bi_{12}GeO_{20}$. The diffusion length is proportional to the square root of the mobility and the lifetime of the photoexcited carriers. By measuring the lifetime and using the diffusion length measurement of Ref. 7, Le Saux, Launey, and Brun[8] inferred a mobility of 130 $cm^2V^{-1}s^{-1}$ for carriers in $Bi_{12}GeO_{20}$. Jonathan, Rossignol, and Roosen[9] measured the build-up time of the photorefractive grating excited by picosecond pulses in $Bi_{12}SiO_{20}$ and deduced the value 50 $cm^2V^{-1}s^{-1}$ for the carrier mobility. Another optical determination of the charge-carrier mobility was performed by Astratov, Il'inskii, and Furman.[10] They studied the growth of electrical screening field through the electro-optic effect and evaluated values from 10^{-9} to 10^{-4} $cm^2V^{-1}s^{-1}$ at temperatures from 130 to 200 K, respectively. At higher temperatures the screening field development was too complicated for the determination of mobility.[11]

Here we report a direct holographic time-of-flight measurement of a photoexcited charge-carrier mobility in an insulator.[12] We find the electron mobility to be 0.24 ± 0.07 $cm^2V^{-1}s^{-1}$ in a previously well-characterized sample of $Bi_{12}SiO_{20}$. We also report transient photocurrent measurements from which we obtain two independent estimates of this mobility, (1) using the absolute value of photocurrent, as in Refs. 3 and 4 (0.13 ± 0.08 $cm^2V^{-1}s^{-1}$), and (2) using the recombination time, as in Ref. 8 (0.17 ± 0.1 $cm^2V^{-1}s^{-1}$). These two qualitative estimates from photocurrent experiments are consistent with our holographic measurement of mobility. In the time-of-flight mobility measurement we use the spatially sinusoidal intensity pattern of overlapping picosecond laser pulses to excite a sinusoidal pattern of electrons into the conduction band, where it drifts under the influence of a strong applied static electric field. The spatially modulated space-charge field caused by the excited electrons and the ions they leave behind is initially zero, grows to a maximum after electrons have moved one-half of the period of the intensity pattern, and fall to a minimum after the full period. We probe the space-charge field with a Bragg-matched cw laser through the electro-optic effect. The electron drift velocity and thus the mobility are calculated from the time required for electrons to drift one period. Pauliat *et al.*[13] recently used a similar kind of method to measure the mobility in $Bi_{12}GeO_{20}$, however, with cw laser excitation and an alternating applied electric field.

We present a simple theory for our holographic time-of-flight technique in Sec. II. Because estimates for mobility and lifetime of photoexcited charge carriers from photocurrent experiments were required to set experi-

mental conditions suitable for the time-of-flight mobility measurement, we describe the transient photocurrent measurements in Sec. III before describing the holographic mobility measurement in Sec. IV. In Sec. V we discuss some implications of the small value of the mobility (compared to drift mobilities in semiconductors), which we measured.

II. THEORY OF HOLOGRAPHIC TIME-OF-FLIGHT TECHNIQUE

We assume that the photorefractive crystal is illuminated with two short interfering laser pulses that are negligibly attenuated, resulting in an energy flux distribution inside the crystal given by (in units of $\mathrm{J\,cm^{-2}}$)

$$U(z)=U_0[1+\mathrm{Re}(me^{ikz})] . \tag{1}$$

Here m is the modulation depth and k is the wave vector of the interference pattern. The laser pulse is considered to be so short that the excited charge carriers may be assumed not to move noticeably in space during the pulse. We will assume that after the excitation, the movement of electrons is described (in the dark) by the following four equations. (Similar equations for holes may be constructed when needed.[14]) First we assume that the ionized donor density $N_D^+(z,t)$ changes only by the single direct recombination process:

$$\frac{\partial N_D^+}{\partial t}=-\gamma N_D^+ n . \tag{2}$$

Here γ is the recombination rate constant. Then, the continuity equation for the density $n(z,t)$ of photoexcited electrons is

$$\frac{\partial n}{\partial t}=\frac{1}{e}\frac{\partial}{\partial z}j-\gamma N_D^+ n , \tag{3}$$

where e is the (positive) charge of the electron. The current density $j(z,t)$ is assumed to consist only of a drift and a diffusion z component near thermal equilibrium at temperature T, so that it can be written in the form

$$j=e\mu nE+\mu k_B T\frac{\partial}{\partial z}n , \tag{4}$$

where μ is the (positive) electron mobility and k_B is Boltzmann's constant. Finally, the Poisson equation for the superposition $E(z,t)$ of Coulomb fields arising from the charged donor density N_d^+ and excited electron density n is, in SI (Système International) units

$$\frac{\partial}{\partial z}E=\frac{e}{\epsilon}(N_D^+-N_A-n) , \tag{5}$$

where ϵ is the dielectric constant and the constant N_A is the density of acceptor sites required to make the crystal electrically neutral in the dark at static equilibrium. At low excitation energy fluxes the initial values of N_D^+, n and E can be written in the same form as the energy flux of (1). Because we consider only the case of small modulation $|m|\ll 1$, we only need to keep terms that are constant in space or that vary as e^{ikz} at subsequent times:

$$\begin{aligned} N_D^+(t,z)&=N_0(t)+\mathrm{Re}[N_1(t)e^{ikz}] ,\\ n(t,z)&=n_0(t)+\mathrm{Re}[n_1(t)e^{ikz}] ,\\ E(t,z)&=E_0(t)+\mathrm{Re}[E_1(t)e^{ikz}] . \end{aligned} \tag{6}$$

Although we may quote parameters in other units, the formulas here will always be assumed to be in SI units.

We will assume that the laser-pulse energy flux U_0 is small enough so that n_0 and n_1 are proportional to U_0. Substituting (6) in (2)–(5) shows that this requires first that $n_0\ll N_A$, so that N_D^+ can be replaced by N_A ($\simeq 10^{16}$ $\mathrm{cm^{-3}}$) in the right-hand side of (2). More stringently, it requires the average density of excited electrons to be much smaller than the saturation density n_s defined by

$$n_s=\frac{\gamma N_A\epsilon}{\mu e}+k^2\frac{k_B T\epsilon}{e^2} , \tag{7}$$

so that we only need to keep terms in (3) that are linear in U_0. In our experiments k^2 is much less than K_e^2 ($\equiv\gamma N_A e/\mu k_B T$), which was found to be 3×10^6 $\mathrm{cm^{-2}}$ in Ref. 14. This gives $n_s\geq 10^{12}$ $\mathrm{cm^{-3}}$. With these approximations (3) and (4) give

$$\frac{\partial n_1}{\partial t}=-\left[\gamma N_A+k^2\mu\frac{k_B T}{e}-ik\mu E_0\right]n_1 , \tag{8}$$

which can be solved immediately. With the same assumptions we get an equation for E_1:

$$\frac{\partial E_1}{\partial t}=\frac{e}{\epsilon}\left[\mu E_0+ik\mu\frac{k_B T}{e}\right]n_1 . \tag{9}$$

With the solution for n_1 from (8) we find a solution to (9):

$$E_1(t)=E_\infty(1-e^{-\Gamma t}) , \tag{10}$$

which satisfies the initial condition $E_1(0)=0$, and in which

$$\Gamma\equiv\Gamma'+i\Gamma''=\gamma N_A+k^2\mu\frac{k_B T}{e}-ik\mu E_0 \tag{11}$$

and

$$E_\infty=-\mu\frac{e}{\epsilon}n_1(0)\frac{E_0+ikk_B T/e}{\Gamma} . \tag{12}$$

It is clear from (11) that the imaginary part Γ'' of the damping constant does not depend on any other material parameters than the mobility itself. If the experimental conditions are arranged to be such that Γ'' is larger than Γ', the temporal oscillation in the amplitude E_1 of the grating electric field becomes visible and the mobility μ can be determined from the oscillation period, i.e., the time it takes for an electron to drift one grating period. From (5) the oscillation is caused by the superposition of the stationary ionic grating upon the grating of electrons drifting with constant velocity under the influence of the strong and applied electric field E_0, with the two space-charge fields canceling each other initially, and at each subsequent time when the gratings coincide. The requirement that Γ'' be clearly larger than Γ' corresponds to the requirement that photoexcited carriers drift at least one

period before experiencing recombination and significant effects from diffusion.

We observe the time development of the space-charge field grating by diffracting a laser beam from it. The diffraction efficiency η is proportional to the square of the amplitude E_1 of the Coulomb grating, so the time behavior of η is, from (10),

$$\eta=\eta_\infty|1-e^{-(\Gamma'+i\Gamma'')t}|^2 , \tag{13}$$

where η_∞ is the value of diffraction efficiency after the oscillations have damped out.

III. TRANSIENT PHOTOCURRENT EXPERIMENTS

We studied photoexcited carriers in a $5\times5\times5$ mm^3 n-type $Bi_{12}SiO_{20}$ single crystal grown by Sumitomo and designated as crystal SU1 in Ref. 14, where it was characterized by fitting quasi-cw two-beam coupling and grating erasure data to the electron-hole competition model. These experiments did not determine the mobility μ and the recombination time τ separately, but only their product. Therefore we first made the following photocurrent measurements to obtain estimates of μ and τ separately, and to predict a useful grating spacing for the time-of-flight measurement.

We studied the decay of the photocurrent induced in the crystal by a uniformly illuminating 30-ps laser pulse when an electric field ($\simeq 1$ kV/cm) was applied to the crystal, which is coated with two conducting electrodes separated by d. At low fluences (≤ 30 μJ/cm^2) the decay of the photocurrent $i(t)$ can be fit by two exponential decays over several orders of magnitude in time and level of signal (as reported in Ref. 3). The time constants for the exponential decays are $t_1=26\pm3$ ns and $t_2=80\pm5$ μs. The faster component displaced about 1% of the charge of the slower one. A convenient way to present the photocurrent data is to express it in the form of the average magnitude $x_a(t)$ of the distance traveled by a photoexcited charge carrier:

$$x_a(t)=N^{-1}\sum_{n=1}^{N}|x_n(t)|=\frac{d}{Ne}\int_0^t i(t')dt' \tag{14}$$

and plot the curves using logarithmic scales. Here $x_n(t)$ is the distance traveled by the nth carrier in the direction of the electric field, and N is the total number of mobile carriers generated by the laser pulse. We estimate N by applying the observation of Ref. 14 that nearly every absorbed photon excites a carrier to our measured absorption coefficient of 0.74 ± 0.25 cm^{-1}. Taking into account the 20% Fresnel reflection at each surface of the crystal, we find the $\ln(x_a)$ vs $\ln(t)$ curve shown in Fig. 1 with the two characteristic shoulders corresponding to the two different exponential decays. The parameters of the two exponentials are consistent with the predictions that one would make assuming the electron-hole model and the parameters of Ref. 14 for SU1, if we take, in addition, the hole and electron recombination times to be, respectively, the t_1 and t_2 of Fig. 1. However, *any* reasonable model would have to associate the longer t_2 with the electrons that are clearly the majority carriers for the photorefractive effect, and the majority contributors for $x_a(\infty)$ in

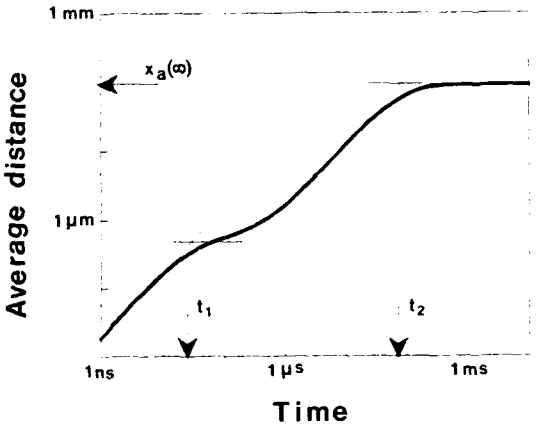

FIG. 1. Average distance $x_a(t)$ traveled by photoexcited charge carriers as a function of time t, calculated by Eq. (14) from our photocurrent measurements at low fluences (≤ 30 μJ/cm^2) and at average applied electric field of 1 kV/cm.

Fig. 1. We see that the majority carriers (electrons) travel about 100 μm, before recombination when the applied electric field is of the order of 1 kV/cm. Therefore we adjust the grating period to be about 100 μm in the experiments of the next section.

We can determine a preliminary value for the electron mobility [$\mu_a=x_a(t)/(E_0t)$] from Fig. 1. Using values for x_a and t just before the second shoulder and taking into account the quantum efficiency of 0.86 for electron excitation[14] we get $\mu=0.13\pm0.08$ cm^{2}V^{-1}s^{-1}. As was mentioned in the Introduction, another, independent estimate of mobility uses the recombination time $t_2=80\pm5$ μs measured here and diffusion length $K_d^{-1}=5.8\pm2.3$ μm reported in Ref. 14 for electrons in the same sample. This gives a value $\mu=0.17\pm0.1$ cm^{-1}V^{-1}s^{-1}.

IV. HOLOGRAPHIC TIME-OF-FLIGHT MOBILITY EXPERIMENT

Our holographic time-of-flight mobility measurement employs the experimental arrangement illustrated in Fig. 2. The interference pattern is written by 30 ps frequency-doubled pulses (at 5 Hz) from a Nd/YAG (yttrium aluminum garnet) laser at the wavelength of 532 nm. The beam expander (BE) creates uniform illumination of the sample. The beam splitter BS1 provides two beams S_1 and S_2. Beam S_1 illuminates a Ronchi ruling R which is imaged on the $Bi_{12}SiO_{20}$ sample by a pair of Fourier-transforming lenses L_1 and L_2. In the intermediate Fourier plane an aperture A selects the two lowest-order components (0 and -1 or 1) diffracted by R. The crystal is thus illuminated by a sinusoidal distribution of intensity whose period is 93 μm and modulation depth $|m|$ is near 1. The writing pulse energy flux was 1 μJ/cm^2 ($n_0\approx1.6\times10^{12}$ cm^{-3}). Beam S_2 is used to erase the previously written gratings by uniformly illuminating the crystal from the back. Two electronically controlled shutters Sh_1 and Sh_2 ensure single-pulse writing of the grating and its erasure. A voltage V_0 is applied to the crystal by a power supply which is electronically switched on just before the writing pulse to minimize

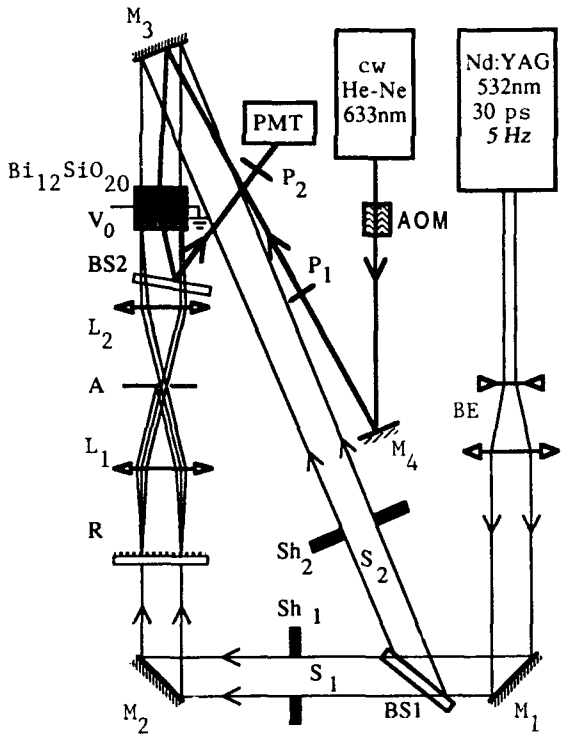

FIG. 2. Experimental arrangement for time-of-flight measurement of mobility of electrons in sample $Bi_{12}SiO_{20}$.

space-charge field buildup. The crystal is oriented so that the grating wave vector is along its (110) crystallographic axis. The diffraction efficiency is monitored using a 10-μW He-Ne laser beam that is linearly polarized by P_1 so that the polarization of the light scattered by defects in the crystal is largely orthogonal to that of the diffracted beam and can be blocked by the polarizer P_2. An acousto-optic modulator (AOM) is used to turn the He-Ne beam on synchronously with the writing pulse from the Nd/YAG laser, and turn it off during the erasure phase. A careful timing allows full decay of the space-charge field between successive writing pulses and minimizes the effect of the photocurrents produced by the He-Ne beam, which is switched on only 200 μs before the writing pulses. A photomultiplier tube (PMT) measures the time evolution of the diffracted signal. The noisy signal is averaged over about 50 shots and filtered both electronically at the input of the storage digital oscilloscope and later numerically. The total integration time of this smoothing process is kept smaller than 0.1 times the time interval between the laser pulse and the diffraction maximum.

Figure 3 shows the experimental time evolution of the diffraction efficiency for SU1 with the voltage $V_0=1$ kV applied across the crystal, along with the best fit of this data to (13) having η_∞, Γ', and Γ'' as fitting parameters. To be able to evaluate the mobility from (13) we must know the value of the applied electric field E_0 inside the crystal. It has been frequently observed that E_0 inside photorefractive materials does not generally equal V_0/d, where d is the distance between the electrodes.[15] We measured the electric field E_0 in a separate experiment

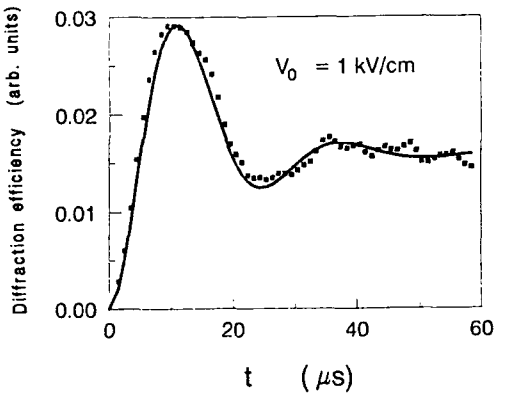

FIG. 3. Time behavior of diffraction efficiency in $Bi_{12}SiO_{20}$ sample after picosecond photoexcitation pulse. The solid curve is a plot of Eq. (13) with $\Gamma'=8.6\times10^4$ s^{-1} and $\Gamma''=2.42\times10^5$ s^{-1}, which gives the least mean-squares error when compared to data.

using the change in the polarization of the transmitted He-Ne beam caused by the electro-optic effect and using the analysis of Ref. 15. The values measured for E_0 were typically 0.7 V_0/d, with the coefficient increasing slightly with V_0. To characterize the uniformity of E_0 across the crystal these measurements were done with a beam diameter of 0.4 mm, one-third of the beam size used for the diffraction experiment. The field E_0 was found to be uniform within 5% both along and normal to the electric-field direction. We also could observe that E_0 did not change more than 5% during the buildup of the photorefractive grating.

The imaginary part Γ'' of the parameter in (11) divided by k is the mean electron drift velocity $\bar{v}$. A plot of the drift velocity $\bar{v}$, obtained from best-fit Γ'' values as a function of E_0 is shown in Fig. 4, demonstrating linear variation and confirming that the photoconduction is Ohmic. From this set of data we obtain a mobility $\mu=0.24$ cm^{2}V^{-1}s^{-1} with the main uncertainty arising from the uncertainty in the average electric field, which we estimate could be as far off from our electro-optic measurement as is V_0/d ($\simeq\pm30\%$). We also found that, contrary to (11), the best-fitting Γ' also varies linearly

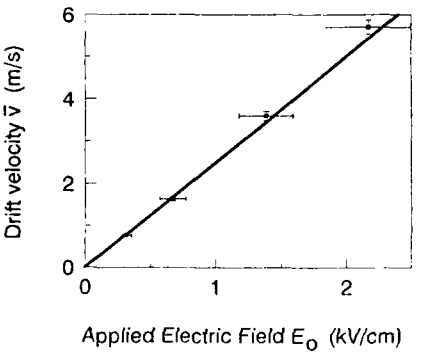

FIG. 4. Mean electron drift velocity $\bar{v}$ vs applied electric field E_0 as determined by fitting Eq. (13) to four curves, such as shown in Fig. 3. $\bar{v}\equiv\Gamma''/k$.

with the electric field E_0 for points of Fig. 4. We have shown that this is consistent with a random variation of mobility ($\pm 40\%$) across the crystal volume.[12]

V. DISCUSSION

The electron mean free path, calculated from the standard expression $[\mu(2k_BTm)^{1/2}/e]$ and our measured $\mu = 0.24\ \mathrm{cm^2\,V^{-1}\,s^{-1}}$, is less than the typical separation of atoms in the crystal lattice. This indicates that the model of collision-limited free-electron transport in the conduction band does not apply to the photoexcited electrons that we are observing. However, our measurements demonstrate that the average drift velocity depends linearly on the applied electric field (Fig. 4) and therefore justifies the concept of mobility. Our low mobility value can be explained as a trap-limited mobility μ_t:[16] Photoexcited electrons do not move in the conduction band continuously. They fall occasionally to an energy level from which they can be thermally excited. The trap-limited mobility is related to the actual conduction-band mobility μ_c by the expression

$$\mu_t = \mu_c \frac{\tau_t}{\tau_t + \tau_r} , \tag{15}$$

where τ_t is the average time spent by a conduction electron between trapping events and τ_t is the average time for a trapped electron before its release. Shallow-trap models have already been used in analyses of charge transport in photorefractive materials.[2-4,10,17]

The wide range of mobility values reported in the literature may also be an indication of trap-limited transport processes: small differences (greater than k_BT) in the depths of traps can indeed lead to an order-of-magnitude difference in thermal excitation rates and thus in trap-limited mobilities. By their nature, shallow-trap events are always dominated by a very narrow energy interval in the gap.[16]

In conclusion, we demonstrate here how a holographic method can be used to measure mobilities of photoexcited charge carriers in photorefractive materials. Using this method on a well-characterized *n*-type $Bi_{12}SiO_{20}$ crystal we found a mobility of $0.24 \pm 0.07\ \mathrm{cm^2\,V^{-1}\,s^{-1}}$ for the electrons. The conductivity caused by these photoexcited electrons was found to be Ohmic over our experimental range of 200–2000 V/cm in the electric field. We also estimated electron mobility values indirectly by two independent ways from transient photocurrent measurements reported here and from previous holographic characterization of the same sample. We found good agreement among all three mobility values.

ACKNOWLEDGMENTS

We want to acknowledge helpful discussions with Dr. M. B. Klein and Dr. R. A. Mullen. This research was supported by the U.S. Air Force Office of Scientific Research, under Contract No. F 49620-88-C-0027, and by the National Science Foundation, under Grant No. ECS-8821507. The Institut d'Optique is "Unité associée au Centre National de la Recherche Scientique No. 14."

*Permanent address: Institut d'Optique, Boîte Postale 147, 91403, Orsay, France.

[1]S. L. Hou, R. B. Lauer, and R. E. Aldrich, J. Appl. Phys. **44**, 2652 (1973).

[2]B. Kh. Kostyuk, A. Yu. Kudzin, and G. Kh. Sokolyanskii, Fiz. Tverd. Tela (Leningrad) **22**, 2454 (1980) [Sov. Phys.—Solid State **22**, 1429 (1980)].

[3]G. Le Saux and A. Brun, IEEE J. Quantum Electron. **QE-23**, 1680 (1987).

[4]I. T. Ovchinnikov and E. V. Yanshin, Fiz. Tverd. Tela (Leningrad) **25**, 2196 (1983) [Sov. Phys.—Solid State **25**, 1265 (1983)].

[5]R. G. Kepler, Phys. Rev. **119**, 1226 (1960).

[6]H. Scher and E. W. Montroll, Phys. Rev. B **12**, 2455 (1975); G. Pfister and H. Scher, *ibid.* **15**, 2062 (1977).

[7]R. A. Mullen and R. W. Hellwarth, J. Appl. Phys. **58**, 40 (1985).

[8]G. Le Saux, J. C. Launay, and A. Brun, Opt. Commun. **57**, 166 (1986).

[9]J. C. M. Jonathan, Ph. Rossignol, and G. Roosen, Opt. Lett. **13**, 224 (1988).

[10]V. N. Astratov, A. V. Il'inskii, and A. S. Furman, Pis'ma Zh. Tekh. Fiz. **14**, 1330 (1988) [Sov. Tech. Phys. Lett. **14**, 581 (1988)].

[11]V. N. Astratov, A. V. Il'inskii, and V. A. Kiselev, Fiz. Tverd. Tela (Leningrad) **26**, 2843 (1984) [Sov. Phys.—Solid State **26**, 1720 (1984)].

[12]J. P. Partanen, J. M. C. Jonathan, and R. W. Hellwarth, Appl. Phys. Lett. **57**, 2404 (1990).

[13]G. Pauliat, A. Villing, J. C. Launay, and G. Roosen, J. Opt. Soc. Am. B **7**, 1481 (1990).

[14]F. P. Strohkendl, P. Tayebati, and R. W. Hellwarth, J. Appl. Phys. **66**, 6024 (1989).

[15]J. M. C. Jonathan, R. W. Hellwarth, and G. Roosen, IEEE J. Quantum Electron. **QE-22**, 1936 (1986).

[16]*Photoconductivity and Related Phenomena*, edited by J. Mort and D. M. Pai (Elsevier, Amsterdam, 1976).

[17]G. Pauliat and G. Roosen, J. Opt. Soc. Am. B **7**, 2259 (1990).